12-2014

Single Cell Biophysics: Applications in Cardiomyocyte Mechanobiology and Stem Cell Mechanotransduction

Benjamin Edward Reese
University of Tennessee - Knoxville, breese1@vols.utk.edu

To the Graduate Council:

I am submitting herewith a dissertation written by Benjamin Edward Reese entitled "Single Cell Biophysics: Applications in Cardiomyocyte Mechanobiology and Stem Cell Mechanotransduction." I have examined the final electronic copy of this dissertation for form and content and recommend that it be accepted in partial fulfillment of the requirements for the degree of Doctor of Philosophy, with a major in Biomedical Engineering.

Mingjun Zhang, Major Professor

We have read this dissertation and recommend its acceptance:

William R. Hamel, Jindong Tan, Mei-Zhen Cui

Accepted for the Council:

Carolyn R. Hodges

Vice Provost and Dean of the Graduate School

(Original signatures are on file with official student records.)

Single Cell Biophysics: Applications in Cardiomyocyte Mechanobiology and Stem Cell Mechanotransduction

A Dissertation Presented for the
Doctor of Philosophy
Degree
The University of Tennessee, Knoxville

Benjamin Edward Reese
December 2014

ABSTRACT

While a great deal of work has been done to analyze cardiac dynamics and mechanics at the organ and tissue levels, there remains much less data regarding these metrics at the single cell level. Additionally, as fields such as regenerative medicine and tissue engineering are beginning to demonstrate greater therapeutic potential, the study and influence of stem cell mechanics on differentiation has become a major area of interest. For these reasons, along with the continued advancement of molecular techniques and assays, there is a growing need to develop functional assays that can integrate and bridge the findings from multiple length scales, incorporating important physical cues with ongoing molecular studies.

In this work, we have utilized various experimental techniques to quantify the altered mechanics and dynamics of individual cardiomyocytes and stem cells in association with various aspects of pathophysiology, toxin exposure, and stem cell differentiation. Through the completion of single cell studies, we have been able to draw significant insight and further relate various components of cellular mechanobiology, such as time-dependent mechanical cues and altered dynamics, with more physiologically relevant and translational research objectives.

Although much more work is still needed, it is clear that this area of research has the potential to impact future studies in a variety of biomedical applications, opening up the possibilities of what can be accomplished with the use of single cell studies and the developing significance of cellular biophysics.

TABLE OF CONTENTS

LIST OF FIGURES

CHAPTER I

INTRODUCTION AND BACKGROUND INFORMATION

Cellular biophysics is an interdisciplinary field, combining aspects of physics, molecular biology, and chemistry, looking to elucidate the fundamental principles and mechanisms that govern cell function and behavior. Much of this research has been driven by the development of novel techniques and instrumentation, providing a direct interface between various areas of cellular, structural, and molecular biology. New and ongoing studies in this field offer innovative approaches and directions for answering some of the challenging cell biological questions that lie between the molecular and macroscopic scales. It is at this level of organization that cellular biophysics can combine and integrate complex genomic, proteomic, and structural information regarding some of the basic processes of cell biology in order to better understand their importance in a physiological context.

Cardiomyocyte Mechanobiology

The dynamics of the cardiac cycle can be described at various levels and scales, ranging from cross-bridge cycling, involving protein interactions, to the resultant periodic contractions of the whole heart. Depending on the parameters of interest and the scale that is being considered, an array of scientific perspectives and techniques can be used to characterize these events. The physical demands of the heart, along with the complex network of molecular signaling that occurs throughout the cardiac cycle, make

this organ especially vulnerable to damage over time. As the heart relies on several mechanisms involving the precise synchronization and coupling of multiple factors, there are a number of ways in which small fluctuations in a single component can cause perpetual alterations in cardiac dynamics, potentially leading to cardiomyopathy and dysfunction. Consequently, much research has been focused on trying to understand the fundamental mechanisms involved in this multifactorial process.

Following the above discussion, the mechanical properties and stresses associated with the dynamic behavior of the heart are closely linked with many of the underlying biological functions taking place throughout this highly regulated and cyclic process. Therefore, various physiological and pathological factors can greatly influence the mechanobiology of cardiomyocytes, both directly and indirectly eliciting changes in cellular biomechanics and cardiac performance. For example, physiological cardiac hypertrophy results from abnormal cardiomyocyte growth in response to intermittent increases in work-load such as during exercise training, which has been shown to improve cardiovascular performance in an adaptive manner [1]. Conversely, pathological cardiac hypertrophy can be caused by a prolonged mechanical stimulus such as hypertension or aortic stenosis triggering a maladaptive response, which can eventually lead to heart failure [1]. The discrepancies between ventricular remodeling that occur in response to a range of physical stimuli illustrates the importance of mechanical cues with regard to the mechanobiological properties of cardiomyocytes, and the role this plays in cardiovascular dynamics.

As shown in the above example, the characterization of mechanobiological properties taken from individual cardiomyocytes offers additional possibilities for studying cardiomyopathy and related pathologies. Although some of these dynamic properties have been well-studied at the organ and tissue levels, more studies are needed to determine the additional parameters that could be elucidated at the level of the cardiomyocyte. Contractility studies have been performed on isolated cardiomyocytes and have shown that certain cardiomyocyte dynamics, such as contractile force and shortening velocity, can be used to correlate similar performance metrics of the whole heart, demonstrating the potential for cellular level studies to provide clinically relevant data on the fundamental mechanisms leading to heart failure [2-4]. As more datasets are becoming available indicating the molecular distinctions between different pathologies, the added level of characterization offered by studies of cardiomyocyte mechanobiology could offer additional insights regarding the transition from a healthy to a diseased state.

The field of mechanobiology attempts to address these physical factors occurring in conjunction with the genetic and molecular markers that have been identified in an effort to better understand the underlying mechanisms associated with pathophysiology. Within this area of research, there are many parameters that can be linked with cellular biomechanics such as the force of contraction, the speed of cell shortening and relaxation, the stiffness or elasticity of the cell membrane, the frequency of beating, and the relationships that exist between all of these parameters in response

to various stimuli [5]. Just as molecular or genetic profiling can be used to describe a specific cardiomyopathy, a functional assay consisting of the above parameters could provide characteristic patterns of behavior resulting from pathological changes [6, 7].

As there are many variables that feed into this complex dynamic network that regulates the cardiac cycle, it is becoming more and more difficult to isolate and control specific parameters of interest. An advantage of cellular studies comes from the enhanced ability to modify and control the environment in a number of different ways to better simulate and study *in vivo* situations in an *in vitro* setting. This limits some of the inherent variability that is associated with animal or clinical studies in order to target the specific changes driving pathophysiology, further making this a viable option for mechanistic studies and the development of experimental models. Additionally, as the heart is under a constant state of fluctuating dynamics, it becomes very important to be able to monitor the response in real-time throughout the time-course of these changes. Cellular studies enable this type of characterization and monitoring, along with the sensitivity to detect fluctuations that might be lost at the level of the whole heart.

In conclusion, much less research has been dedicated towards analyzing the physical parameters associated with cardiomyopathy and dysfunction, even though the principal function of the heart relies on the coupling of mechanical and molecular dynamics. Cardiomyocytes represent a group of cells that are constantly exposed to fluctuating levels of mechanical stress, stemming from various biological factors that influence the extent to which these cells must continuously adapt. In an effort to

quantify some of the underlying mechanobiological properties of cardiomyocytes, the following research applies a combination of physical and molecular techniques in order to elucidate some of the fundamental mechanisms leading to pathophysiology and disease.

Excitation-Contraction Coupling (ECC)

Excitation-contraction coupling at the single cell level involves both molecular cues from various voltage gated ion channels, in conjunction with cross-bridge cycling that generates the physical shortening of cardiomyocytes in response to fluctuating currents and the availability of various protein interactions [8].

This fundamental process of cardiomyocytes is initiated by an action potential which results in the rapid depolarization of the sarcolemma through t-tubules. During the action potential, a transient increase in cytosolic calcium enables the shortening of sarcomeres due to actin-myosin interactions. Following the subsequent repolarization of the cell, calcium is rapidly effluxed from the cytosol, causing the relaxation and re-lengthening of cardiomyocytes. Based on this tightly regulated cycle, cardiomyocytes are able to quickly respond to external cues in order to meet the physical demands of the heart. This relationship illustrates some of the mechanobiological properties of cardiomyocytes that can greatly influence cardiac function.

Calcium-Induced Calcium Release (CICR)

As previously described, the cardiac cell cycle is a calcium-regulated dynamic process relying on calcium-induced calcium release (CICR), in order to generate the cyclic and periodic contractions of the heart [9]. Any alterations in the timing or molecular kinetics that occur during this process can lead to significant changes in contractility and cardiac performance.

The transient rise in cytosolic calcium concentration is due, in large part, to calcium-induced calcium release (CICR) from the sarcoplasmic reticulum (SR). The bulk of calcium originates from the SR, which stores calcium within the cardiomyocyte. However, the initial influx of calcium through L-type calcium channels triggers this release from the SR. Additionally, the activation of ryanodine receptors (RyRs) located on the SR plays a major role in this process, as alterations to these calcium channels can affect the concentration and speed with which calcium is released into the cytosol.

Multi-Scaled Dynamics and Mechanics

Cardiomyocyte dynamics and mechanics help to bridge the scale between myofibrils within the cell, made up of sarcomeres, to the multi-cellular tissue-level coordination seen in the myocardium [10]. It is important to consider the role that individual cardiomyocyte mechanics and dynamics have on the same metrics of the whole heart.

As previously mentioned, correlating the molecular mechanisms driving these functional changes at the cellular level will help to elucidate the ways in which pathological changes, cardiotoxic drug effects, and genetic alterations cause damage at the tissue and organ levels. The insight provided from cell studies could then offer better solutions of translational significance for the preventative, diagnostic, and therapeutic strategies used in a clinical setting.

Stem Cell Mechanotransduction

It is well known that biochemical signals play an important role in stem cell differentiation and embryonic development. However, recent evidence has shown the effects that mechanical cues can have on a variety of mechanisms that regulate stem cell biology [11]. The ability for cells to convert mechanical stresses into biochemical signals still holds great potential for many therapeutic applications in the fields of tissue engineering and regenerative medicine. Stem cells are especially vulnerable to these effects due to their pluripotency and the array of environmental cues that are known to be involved in regulating this fundamental process.

In the same way that electromechanical coupling in cardiomyocyte mechanobiology involves both physical and molecular dynamics, stem cell mechanotransduction is the relationship between physical forces and a complex network of molecular signaling. There is a growing amount of evidence that mechanical triggers can stimulate and even direct stem cell differentiation, with cell fate showing a

preference towards those cell types *in vivo* that mirror the existing conditions *in vitro*. For example, stem cells grown on very stiff substrates tends to produce greater osteogenic differentiation [12], as the stiffness of the *in vitro* environment more closely mimics that of bone *in vivo*.

Due to the importance that physical and mechanical cues have demonstrated in stem cell biology, the ability to measure and quantify this component of mechanotransduction has become increasingly more significant. Acting as one of the toughest challenges facing stem cell use, the ability to control and regulate their growth and differentiation relies, at least partly, on the ability to recreate environmental conditions similar to those found *in vivo*. The following studies regarding stem cell mechanics and differentiation will allow for the isolation and quantification of those effects resulting from a combination of physical and molecular cues.

Stem Cell Differentiation

As mentioned, stem cells are pluripotent in nature and can differentiate into multiple cell types depending on several environmental factors, including both biochemical signaling and mechanical cues. Because of the complex dynamics and signaling that is involved, there are still many aspects of embryonic development that remain unknown. In order to try and better understand those mechanisms driving the process of differentiation, it is important to not only factor in the biochemical cues but also quantify the physical components that are involved. The recent advances in

instrumentation and technology have enabled more studies regarding mechanotransduction and the ways in which this phenomenon is involved in stem cell differentiation. Not only has mechanical stress been able to stimulate and partially direct differentiation, but more recently, a study was able to demonstrate its potential role in reprogramming mammalian somatic cells and inducing pluripotency, which could have major implications in future disease and pathology research [13].

Stem Cell Therapy

As advances are being made in the fields of regenerative medicine and tissue engineering, the safety and efficacy of stem cell therapeutics remains a major challenge. Although the regenerative and restorative properties of stem cells offer several advantages, these cell types are also difficult to control and can form malignant tumors leading to cancer risk when implanted or injected into the body [14]. An application for stem cell therapy includes replacing damaged tissue, which could be used to treat diseased or injured cells. The ability for stem cells to self-renew offers potential in organogenesis and tissue engineering applications, such as skin grafts and myocardial tissue repair where multiple cell types are needed in order to recover functional tissue. With all of the potential that stem cell therapy has demonstrated, the challenges presented have kept its clinical applications to a minimum.

CHAPTER II

EXPERIMENTAL TECHNIQUES AND INSTRUMENTATION

This work includes the use of various experimental techniques and microscopic platforms in order to quantitatively characterize the mechanobiological properties of individual cardiomyocytes and stem cells. Examples of these instruments include the atomic force microscope (AFM), Nanoindenter, Laser Scanning Confocal Microscope (LSCM), and Digital Holographic Microscope (DHM), as well as various other components used to regulate and control experimental conditions such as an environmental chamber and electrical stimulator.

Atomic Force Microscope (AFM)

Atomic force microscopy (AFM) is a physical imaging technique that can be used to obtain high-resolution topographical images, in addition to characterizing certain physical properties of both biological and non-biological samples. The AFM (Asylum MFP-3D BIO) used in this work is mounted on an Olympus IX-81 inverted optical microscope, allowing for its potential integration with other imaging modalities. The quantification of various mechanical properties such as stiffness or Young's modulus can be measured using nanoindentation. In addition to these more traditional techniques, this system is capable of performing various other specialized functions such as nanomanipulation, force spectroscopy, conductive probe microscopy, and nanolithography. Specific areas in which these techniques can be applied include the

real-time monitoring and characterization of beating cardiomyocytes, the mechanobiology of stem cells, and long term studies looking at the effects of various stimuli. In addition to the wide range of applications from materials science to biology, this technique can also be used under a variety of conditions, including ambient air, ultra high vacuum, and in liquids, making this especially useful for biological samples. This AFM setup is also equipped with a perfusion chamber allowing for the precise control over various environmental factors when performing live cell studies. Using this tool, we are able to characterize morphological and material properties of nanostructures, nanomaterials, and biological samples at a level of quantification surpassing that of other conventional microscopic techniques.

Dwell Curves

In order to acquire cardiomyocyte dynamics regarding contractility and the associated beating parameters, a similar technique to that previously described was utilized [4]. In the previous work, this technique was used at multiple points on spontaneously activated stem cell-derived cardiomyocytes in order to generate a "dwell map" showing spatial variations in the acquired parameters. In this work, however, measurements were taken from a single point on the cell's surface (center of contraction) and is referred to as a dwell curve, shown in **Figure 1**.

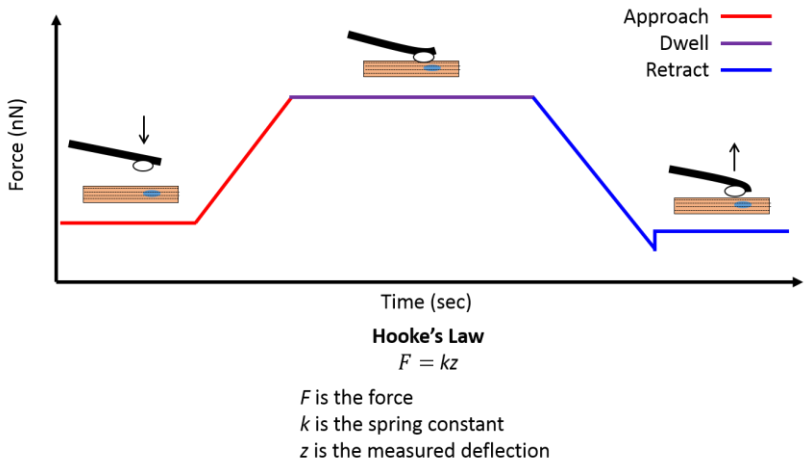

Figure 1. Illustration showing the acquisition of a single dwell curve, along with the equation for calculating force from the deflection signal of the AFM cantilever.

In brief, the AFM was used to passively acquire the beating dynamics of individual cardiomyocytes [15]. This is accomplished by bringing the AFM cantilever into contact with the surface of the cell and fixing the AFM's z-position. By doing so, the contraction of the cardiomyocyte will cause subsequent deflections in the cantilever enabling the monitoring of various beating dynamics as shown in **Figure 2**.

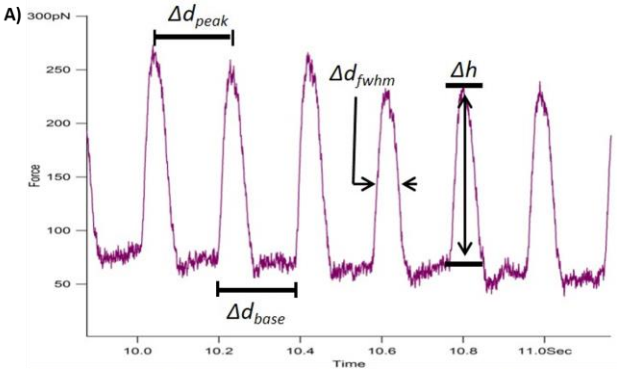

Figure 2. Beating dynamics from the "dwell" portion of a single dwell curve. A) Labeled parameters of interest from force trajectory. B) Parameter definitions.

Nanoindenter

The nanoindenter is among the leaders in advanced indentation and hardness testing for small-scale applications. While our MFP nanoindenter is an AFM-based indenter, it does not use cantilevers as part of the indenting mechanism, providing a substantial advantage in accuracy, precision and sensitivity over other nanoindenting systems. This system is ideal for a variety of nanoindenting applications, such as characterizing the mechanical behavior of thin films, bone, and biomaterials; time-dependent mechanical characteristics of soft and hard materials; and combined nanoindenting with current-voltage measurements. This technique is particularly suited for the dual acquisition of time-dependent mechanodynamics from single cells.

Nanoindentation

In order to determine Young's Modulus for a given sample, a technique termed nanoindentation was performed on the cell's surface (**Figure 3**), utilizing either the AFM or Nanoindenter. This technique produces force curves that can then be further analyzed using Hertz theory to calculate a measure of elasticity or stiffness for the individual or aggregated cells of interest. As the cantilever tip contacts the sample, the interaction between the two surfaces produces a force curve (force vs distance) from which the slope of this curve can then be used to quantify the relative stiffness of the sample.

Triggered force curves allow the user to define the maximum force with which to apply on the sample before the cantilever is retracted. This allows for more consistency when combining data from several samples, and also minimizes the amount of damage to both the sample and the cantilever tip. For example, by defining a trigger force of 1 nN, the AFM cantilever would then approach the surface at a given velocity over a pre-defined distance until contact is made and the deflection signal reaches a value equal to 1 nN of force.

The tip geometry and its material properties are very important for accurately representing the interaction between the AFM cantilever and the cell's surface. For the purposes of this work, a spherical tip was used in order to remove some of the variability and difficulties in the calculation of Young's modulus that can come from using more complex geometries. By using a spherical tip, this also ensures a more uniform and reproducible interaction without causing damage to the cell, which can sometimes be a problem when using a sharp tip on soft biological samples. Another important consideration is the stiffness of the cantilever relative to the sample. Using a softer cantilever provides more sensitivity over a lower range of expected force values (10^1-10^2 nN). This also minimizes the damage that might occur to the cell surface by using a relatively low spring constant cantilever (0.02 – 2 N/m).

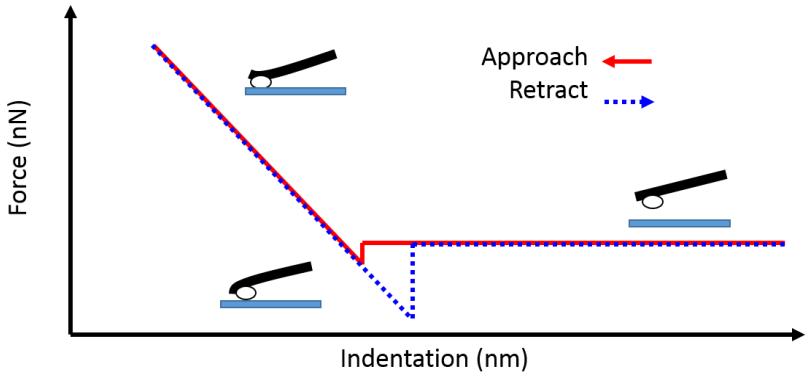

Young's modulus

$$E = \frac{FL_o}{A_o \Delta L}$$

E is the Young's modulus (modulus of elasticity)
F is the force exerted on an object under tension
A_0 is the cross-sectional area through which the force is applied
ΔL is the amount by which the length of the object changes
L_0 is the original length of the object

Figure 3. An illustration showing the acquisition of a force curve, also known as nanoindentation. The equation for calculating Young's modulus is also shown.

Once the force curves are acquired, the use of a built-in software package can then be used to extract the desired parameters of interest. In this work, a Hertz model was used to calculate Young's modulus from the data, as shown in **Figure 4**.

Depending on the sample and the design of the experiment, the contact portion of the force curve can be fitted over a specific region of interest. The stiffness can therefore be determined over a confined range of either force or indentation depth. It is also important to perform a range of force curves in order to ensure that the correct force and indentation depth are being used to remove any unwanted influences from the underlying substrate.

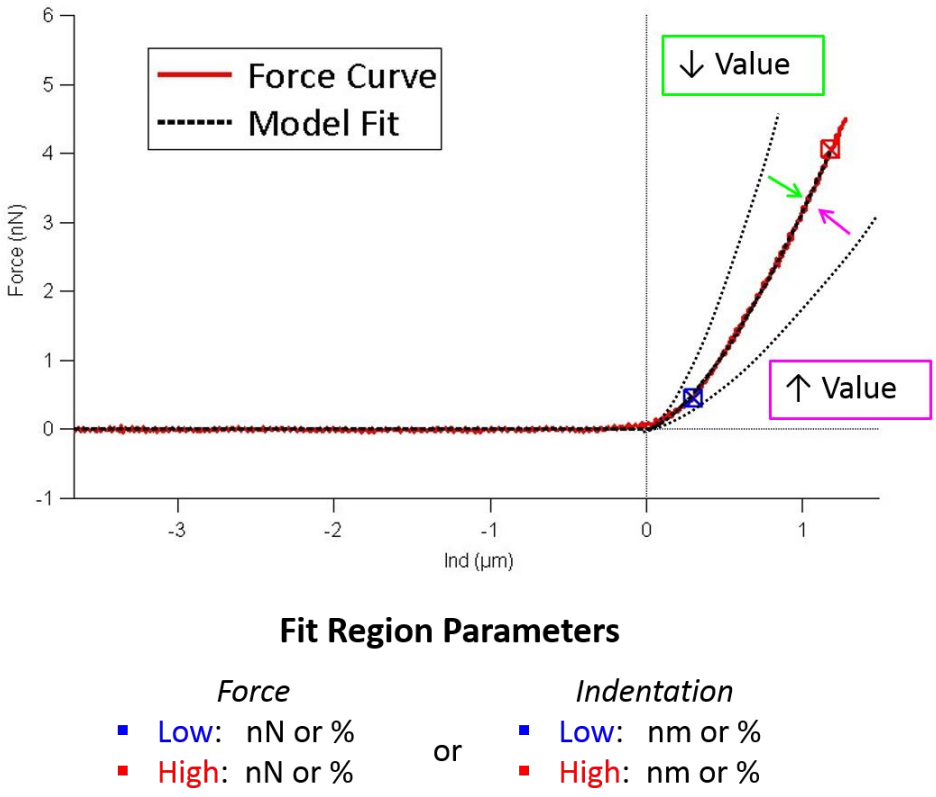

Figure 4. The use of built-in software is used to calculate Young's modulus. Some of the fitting parameters can be manipulated in order to confine the contact portion of the force curve, allowing for the calculation to be completed within a desired range of either force or indentation depth.

Laser Scanning Confocal Microscope (LSCM)

The FV1000 enables high resolution, multi-dimensional observation and analysis of both fixed and living cells and tissues, as well as the ability to perform precise co-localization studies. This system is integrated onto the Olympus IX-81 inverted microscope, equipped with 6 lasers including 4 gas (multi-line Argon 458nm, 488nm, 515nm and HeNe 543nm), and 2 diode (405nm and 635nm) lasers. As with all confocal microscopes, this system uses point illumination and a pinhole to eliminate the out-of-focus signal associated with the unfocused background portion typically seen in

conventional wide-field fluorescence microscopes. This allows for the visualization of specifically labeled internal cellular structures, with the ability to perform time-lapse imaging over long time scales for tracking intracellular movements with its advanced z-sectioning (3D) capabilities. Other features include a motorized z-drive allowing 0.01 micron step increments for focusing and automated sectioning capabilities built into the software. Some applications of this microscope include visualization of drug delivery probes and/or their specific targets, both on the cell surface and/or within the cells of interest, tracking of small particles (nanoparticles ~70nm and larger), and the formation or reorganization of various cytoskeletal elements or structural proteins of interest.

Line-scanning

As described previously, calcium dynamics are an important aspect of cardiomyocyte excitation-contraction coupling. In order to quantify the intracellular calcium dynamics of individual cardiomyocytes, a technique called line-scanning was used [16].

This method of imaging restricts the region to be scanned by a laser scanning confocal microscope to a single line, enabling the rapid acquisition of fluorescent images in sequence with enough temporal resolution to characterize the dynamic fluctuations of calcium levels within the cell over the selected region of interest, as shown in **Figure 5**.

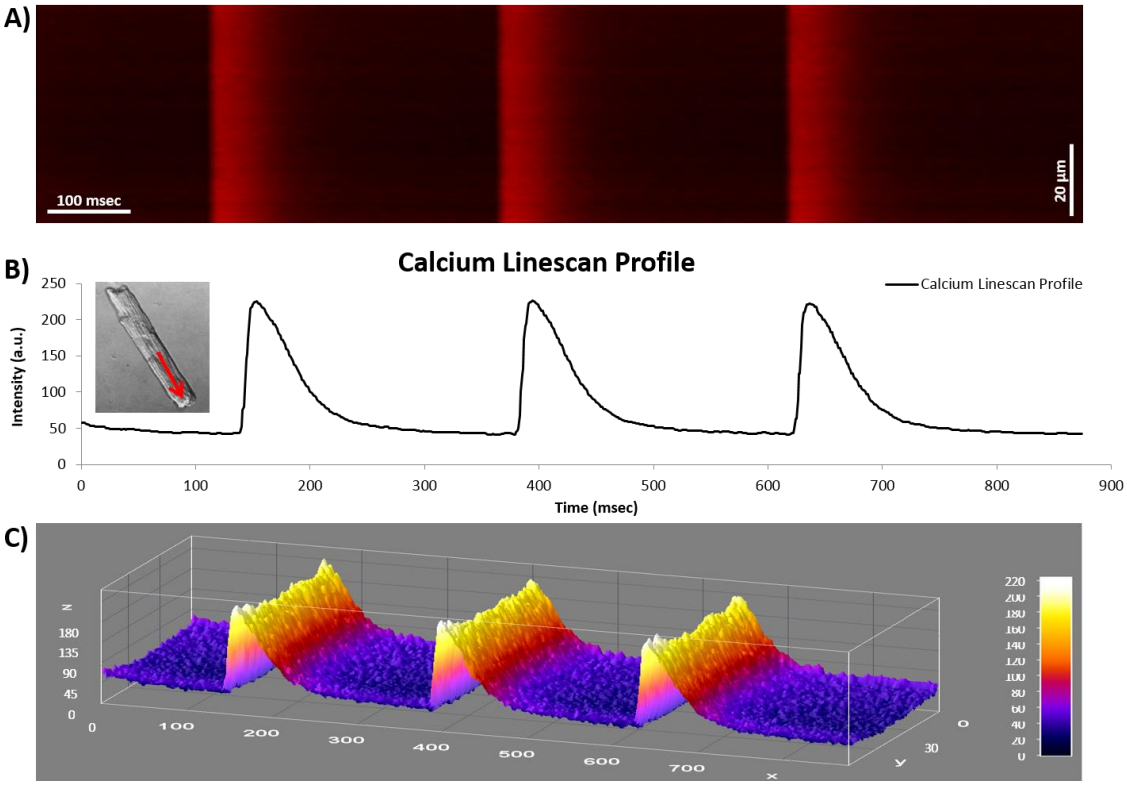

Figure 5. Confocal line-scanning technique used to quantify intracellular calcium dynamics. A) Confocal line-scan of fluorescent intensity, showing distance along the region of interest vs time. B) Profile analysis of the confocal line-scan data shown in (A). C) 3D profile of the confocal line-scan data taken from (A).

A calcium-specific fluorescent dye is introduced into the cell medium and is used to label the calcium, causing it to emit a fluorescent signal in response to stimulation by a laser of a specific wavelength. Several measurements are taken on controlled buffer solutions of known calcium concentration, which then allow for the ratiometric comparison and correlation of fluorescent intensity with calcium concentration. Using this technique, the calcium dynamics of individual cells can then be measured and analyzed in conjunction with the other parameters of interest.

Digital Holographic Microscope (DHM)

The DHM T1000 enables nanometer axial resolution in real-time using non-invasive three dimensional full-field acquisition (no scanning). This technique uses a CCD camera to record a hologram which is then transmitted to a computer in order to digitally reconstruct the image in 3D. The intensity and phase information are decoupled in order to generate data for both the morphology and refractive index of the sample. This system also incorporates a fluorescence module which allows the simultaneous acquisition of morphological shape changes, co-localization studies, and concentration based data generated by the intensity profile of the measured fluorescent signal. Particle or cellular tracking in three dimensions can also easily be monitored, aided by the use of digital focusing provided within the Koala software. There are several exciting areas in which this technology can be applied, including the three dimensional tracking of motile cells or structures without the need for disturbing the natural environment or complex labeling steps, dynamic morphology and/or size/shape changes in response to various stimuli, time-lapse monitoring of various cellular processes such as cardiomyocyte beating or stem cell differentiation, as well as 3D particle tracking in complex fluidic environments, generating 3D velocity profiles.

Phase Monitoring

As both the phase and intensity are collected when capturing an image with the DHM, the ability to monitor phase changes over time allows for data other than 3D morphology to be extracted and analyzed (**Figure 6**).

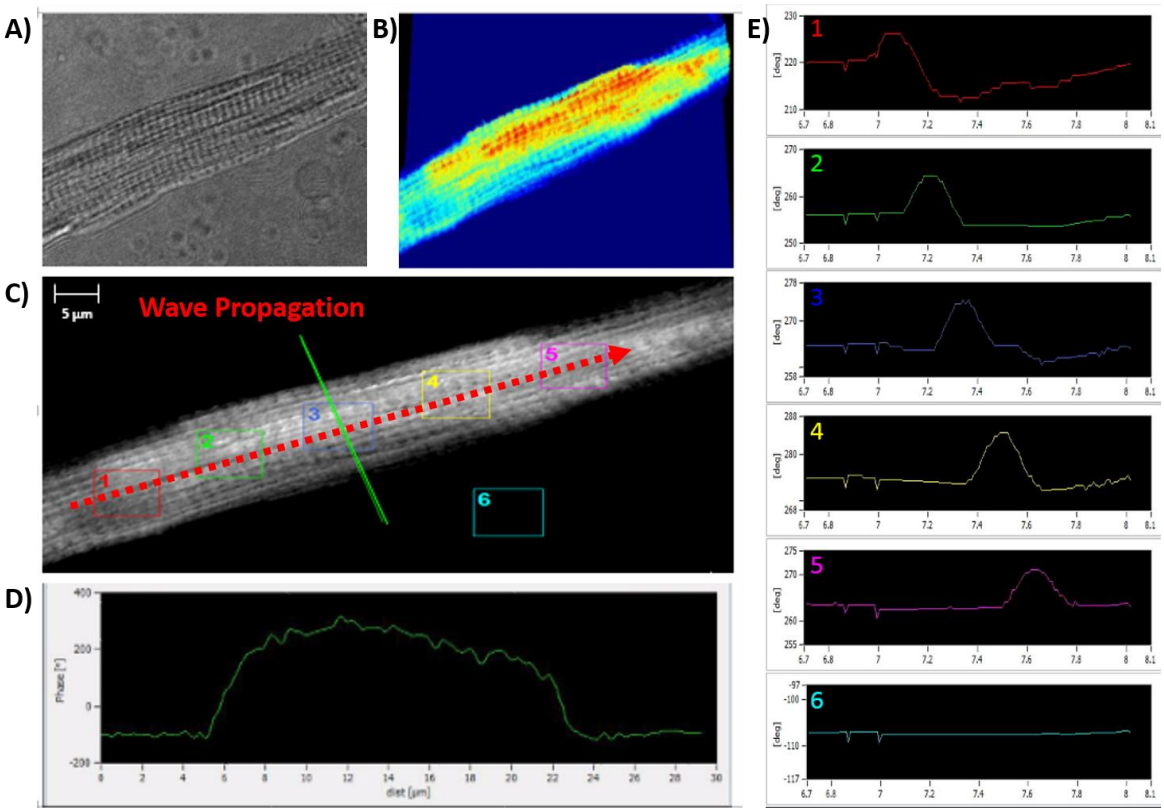

Figure 6. Data from a spontaneously active cardiomyocyte, acquired by the DHM. A) Intensity image of an adult mouse ventricular myocyte. B) 3D reconstruction of phase image in (C). C) Phase image with selected regions of interest (boxes 1-6) for monitoring the phase change over time, as well as a line drawn over the cell to generate a profile as shown in (D). D) Phase profile for the line segment shown in (C). E) Respective phase monitoring corresponding to the selected regions shown in (C) as a wave was propagating along the cell's length.

One of the built-in functions provided by the Koala software package includes phase monitoring. This can be accomplished by selecting a region of interest from a recorded image sequence. An average phase value is then reported for the selected region of interest, and is plotted versus time in a separate graph. This allows for highly localized dynamics to be recorded using this non-invasive technique, providing useful time-course data.

CHAPTER III

MATERIALS AND METHODS

Cardiomyocytes

Adult Mouse Ventricular Myocyte Isolation

Single ventricular myocytes were obtained from adult mice using an enzymatic digestion technique adapted from previous reports [17]. The animals were first heparinized and anaesthetized with methoxyflurane. Upon cervical dislocation, hearts were removed and mounted on a Langendorff apparatus where they were perfused for 5 min with normal Tyrode's solution containing (mM): 130 NaCl, 5.4 KCl, 1 $CaCl_2$, 1 $MgCl_2$, 0.6 NaH_2PO_4, 10 Hepes and 5 glucose (pH adjusted to 7.4 with NaOH). The hearts were then perfused for 10 min with Ca^{2+}-free Tyrode's solution, followed by a 30 min perfusion with Ca^{2+}-free Tyrode's solution containing 73.7 U/ml type II collagenase (Worthington Biochemical Corp.), 0.1% bovine serum albumin (Sigma-Aldrich), 20 mM taurine and 30 μM $CaCl_2$. This was followed by 3 min of perfusion with a KB solution containing (mM): 100 potassium glutamate, 10 potassium aspartate, 25 KCl, 10 KH_2P0_4, 2 $MgSO_4$, 20 taurine, 5 creatine base, 0.5 EGTA, 5 Hepes, 1% BSA and 20 glucose (pH adjusted to 7.2 with KOH). The hearts were then removed from the Langendorff apparatus and the ventricles were excised. Following removal of the ventricles, the tissue was gently triturated with a Pasteur pipette for 10-15 min. Rod-shaped single

myocytes were then collected and either plated immediately or stored in KB solution at 4 °C until use.

Electrical Stimulation

Adult mouse ventricular myocytes are quiescent upon isolation, and therefore need electrical stimulation to induce contractions *in vitro*. A Grass SD9 neurophysiological stimulator was used to generate short pulses (10-30 V @ 4 msec) while connected to platinum stimulation electrodes submerged within the environmental chamber or petri dish housing the isolated cardiomyocytes. Depending on a combination of parameters from the experimental setup, the minimum threshold voltage and pulse duration was found to induce contractions while minimizing the effects and disturbances to the AFM cantilever.

Stem Cells

Cell Culture

For Mg53 treatment studies, primary rat mesenchymal stem cells (MSCs) were isolated from the bone marrow of healthy male rats (220-250 g). Cells already at passage 3 were aged in normal growth medium consisting of α-Minimal Essential Medium (MEM, Gibco), penicillin (50U/ml) (all from Sigma–Aldrich), platelet-derived growth factor (PDGF) (10ng/ml, R&D), epidermal growth factor (EGF) (10ng/ml, R&D) and 2% fetal bovine serum (FBS) (Hyclone) maintained at 37°C in a humidified (5% CO_2:95% air) atmosphere.

For matrix encapsulation studies, R1 murine embryonic stem cells (ESCs) with and without green fluorescence protein (GFP) were purchased from ATCC (Manassas, VA, USA) and cultured in feeder-free medium made of Knockout® DMEM supplemented with 15% Knockout® serum, 1000 U/ml leukemia inhibitory factor, 4 mM l-glutamine, 0.1 M 2-mercaptoethanol, 10 μg/ml gentamicin, 100 U/ml penicillin, and 100 μg/ml streptomycin in gelatin coated tissue culture flasks with daily medium change.

Mg53 Treatment

To study the effects of Mg53 on fresh stem cell differentiation, stem cells were subsequently seeded at a density of 400,000/per well in 6-well culture plates and grown in DMEM medium without PDGF and EGF in the presence or absence of Mg53 (50μg/mL) (Cayman chemical, Cambridge Bioscience). Phosphate buffered saline (PBS) was used as the control solution. Cells were then maintained in continuous culture for 7 to 14 days, before being removed for studies to assess differentiation and membrane stiffness/elasticity.

Matrix Encapsulation

To encapsulate the ESCs in microcapsules with a liquid core and hydrogel shell, they were detached from the flasks using 1x trypsin/EDTA, following a wash in PBS, and then suspended at 5×10^6 per ml in 0.25 M aqueous mannitol and 1% (w/v) sodium carboxymethyl cellulose as the core solution. A coaxial electrospray system was used, including coaxial needle, pumps, voltage generator and collecting bath. In brief, the

core solution was pumped through the inner lumen (28G) of the coaxial needle at 47 µl/min, while the shell solution consisting of 2% purified alginate (w/v) in 0.25 M aqueous mannitol solution was pumped through the outer lumen (21G) at 60 µl/min. Concentric drops generated by core and shell fluids are then broken up into microdroplets under a 1.8 kV electrostatic field and sprayed into the gelling solution made of 100 mM calcium chloride in deionized water. The high viscosities of core and shell solutions, as well as the instant gelling kinetics of alginate, ensured negligible mixing between the two aqueous solutions and therefore resulted in the formation of core-shell microcapsules. After encapsulation, the microcapsules with ESCs were washed with 0.5 M mannitol solution and cultured in ESC medium requiring a daily medium change. All cells were cultured at 37 °C in a humidified 5% CO_2 incubator.

CHAPTER IV

PLATFORM INTEGRATION AND DEVELOPMENT

The initial platform integration and development was designed for studies on cardiomyocyte mechanobiology and were, therefore, conducted on the HL-1 spontaneously active cardiomyocyte culture. Due to several differences between preliminary experiments using cultured cardiomyocytes and the eventual use of isolated adult ventricular myocytes, further development was needed in order to enable the use of the previously described techniques. The next few sections will address the changes that were made, along with the optimization of the protocols used for the remainder of these studies.

Cardiomyocyte Selection Criteria

One of the major differences between the HL-1 cell line and isolated adult ventricular myocytes is their size. While HL-1 cells are much smaller and grow in clusters, adult ventricular myocytes are much larger and can be easily isolated as single cells. Preliminary experiments comparing adult rat cardiomyocytes were designed to look at whether size could be used to predict the relative force of contraction. Two spontaneously active cells were found side by side and each cell was monitored in order to compare the average force of contraction produced in response to variable loading conditions. One cell was much larger than the other, while the smaller cell's sarcomeric organization was visibly enhanced relative to that of the larger cell (**Figure 7**).

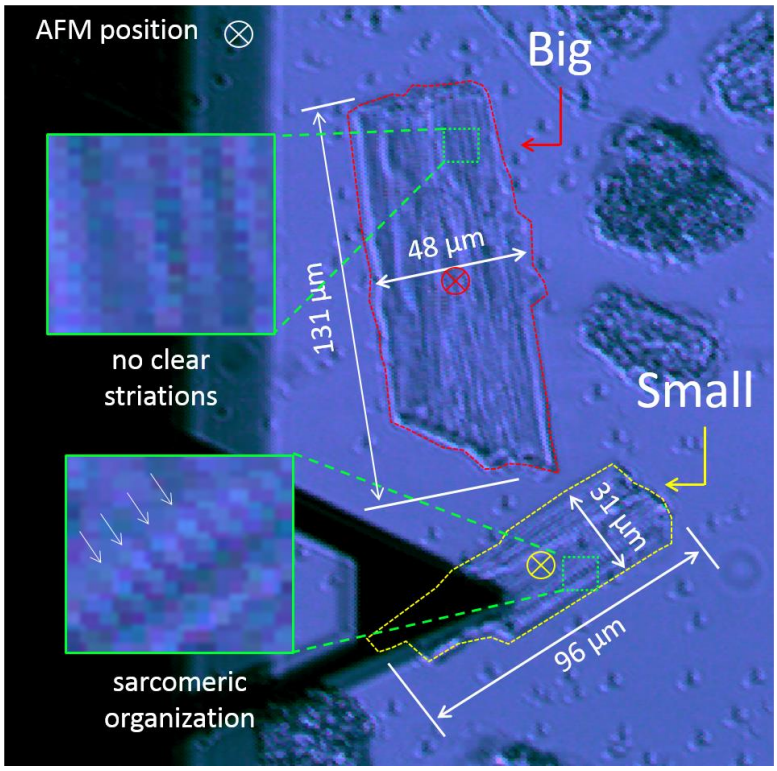

Figure 7. Experiment looking at the influence of size, trigger force, and striation patterning on the force of contraction. The larger cell had no clear striations, while the smaller cell had much better sarcomeric organization.

The results were able to show that sarcomeric organization had a much greater influence on the force of contraction compared to size. As shown in **Figure 8**, on average, the smaller cell was able to generate nearly twice the amount of force compared to the larger cell regardless of the loading conditions. Another conclusion from this study was that there is a positive correlation between the applied force and the resulting force of contraction. This relationship is illustrated in **Figure 9**.

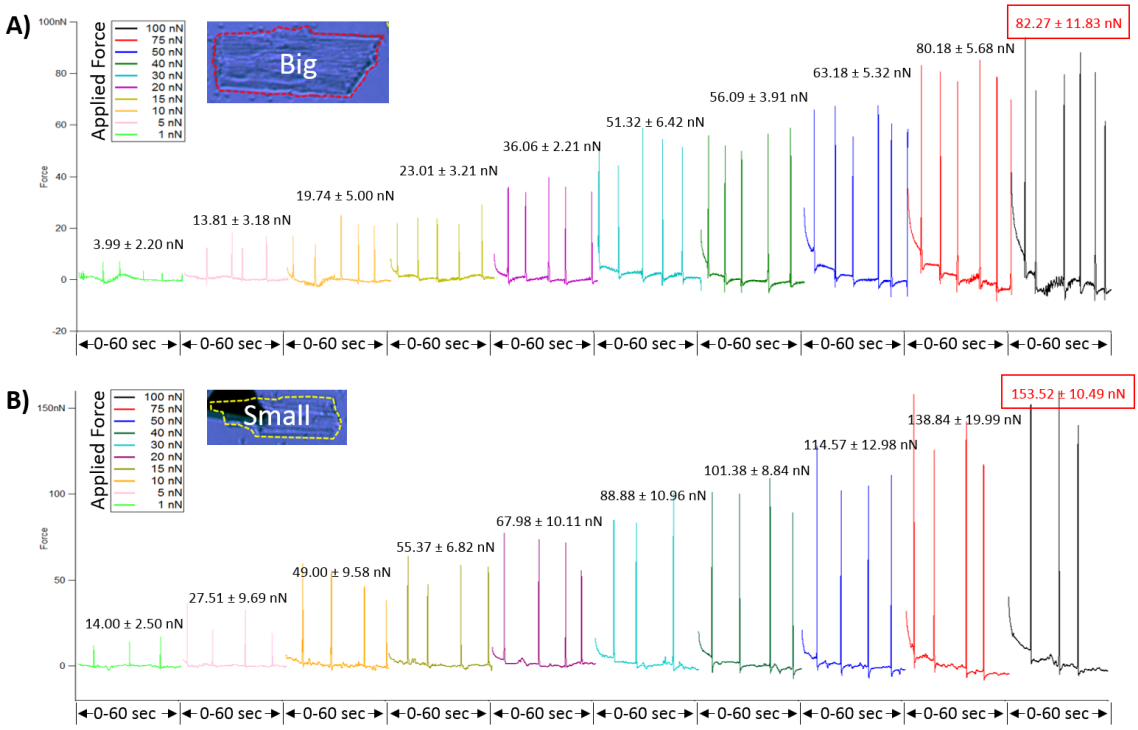

Figure 8. Graph showing the force of contraction at varying applied loads. A) The resulting "dwell" portions of dwell curves from the larger cell in response to varying loading conditions (1-100 nN). B) Results from the smaller cell under the same loading conditions in (A).

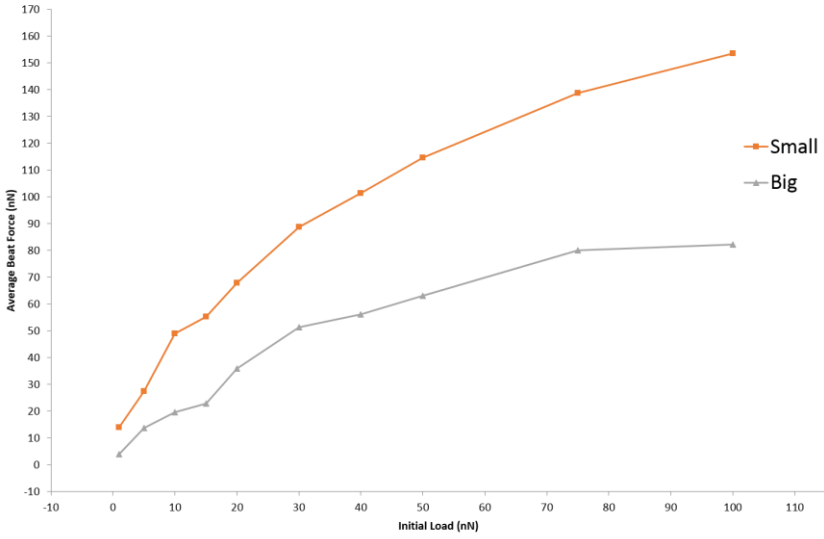

Figure 9. Graph showing trend of applied load versus the resulting force of contraction for both cells from Figure 8.

Optimization and Analysis

Another component that had to be integrated into this system was electrical stimulation. While the HL-1 culture was spontaneously active, adult ventricular myocytes are typically quiescent or can have unpredictable spontaneous activity. Due to the variability in the range of forces produced from cell to cell, and the inconsistencies in beating frequency, using an electrical stimulator to induce contractions was able to remove some of the inconsistencies by generating a much more stable response as shown in **Figure 10**.

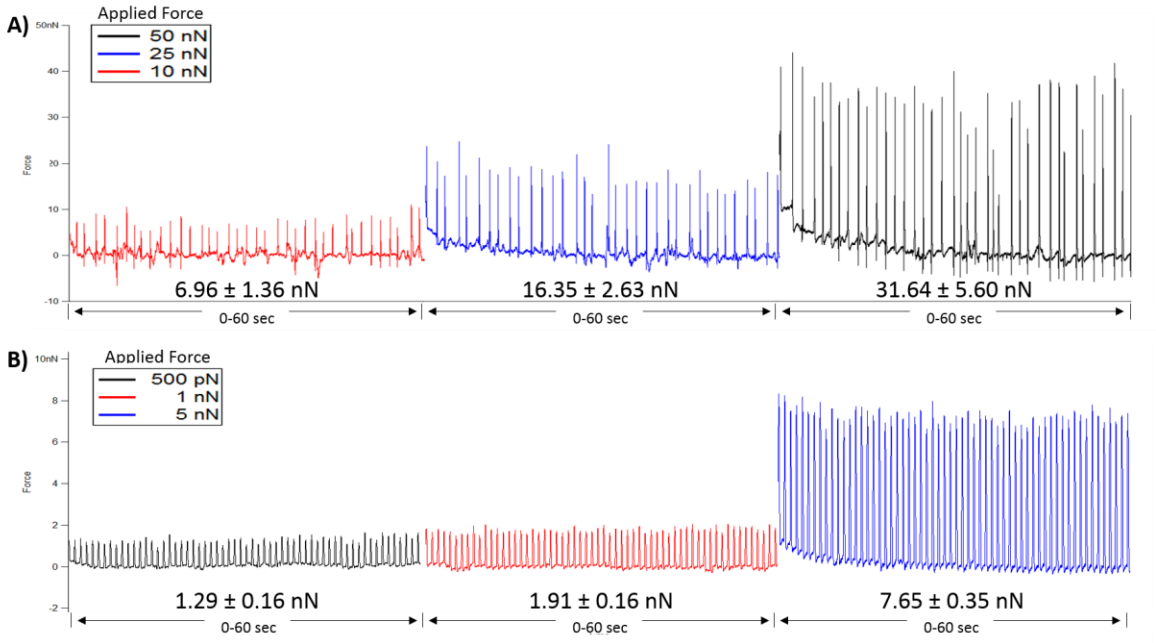

Figure 10. Comparison of the response from a spontaneously active cell versus an electrically stimulated cell. A) The force of contraction at varying loads showing a high standard deviation. B) The results from a stimulated cell showing a much lower standard deviation relative to the spontaneous cell in (A).

In addition to the dynamic characterization of cardiomyocytes, the mechanics of the cell membrane over time were also of interest. An initial study was designed to look at the effects of stimulation on membrane rigidity using the nanoindenter, as shown in **Figure 11**. These results emphasize the importance and advantages of real-time monitoring for performing single cell studies on cardiomyocyte mechanobiology.

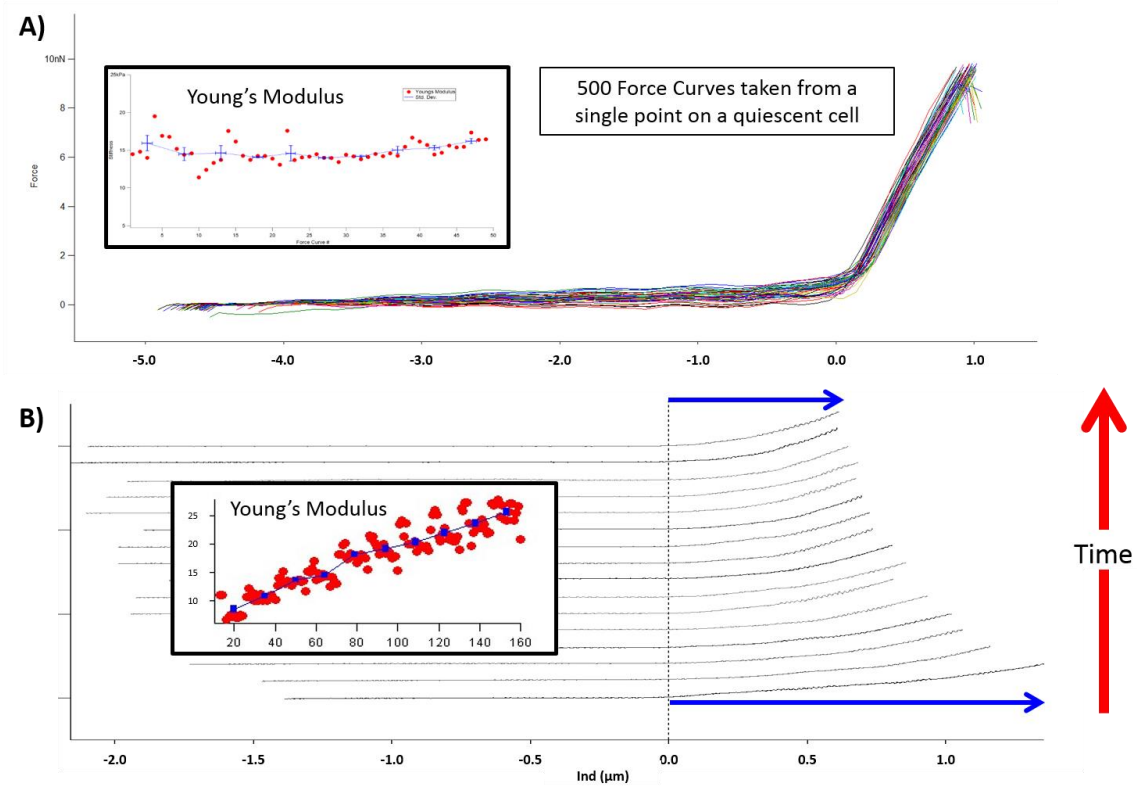

Figure 11. Stiffness comparison for adult ventricular myocytes with and without stimulation. A) Force curves taken over time showing a stable trend in Young's modulus for a quiescent, non-stimulated cell. B) Resulting force curves taken from a stimulated cell, showing an increase in stiffness over time as can be seen by the reduced indentation depth using a fixed trigger force.

With stimulation, there is a steady increase in stiffness of the sarcolemma over time, coupled with more variability. Without stimulation, the resulting stiffness values

are more consistent and stable over the same time period. This might be the result of a gradual increase in intra-cellular calcium over time due to potential electroporation or damage to the cell membrane caused by electrical stimulation. This could also be due to potential cytoskeletal remodeling or enhanced sarcomeric organization occurring in response to continuously eliciting contractions.

Further optimization and preliminary studies led to the integration and development of each component used for the remainder of these studies. A sample data set following the optimized procedure is shown in **Figure 12**.

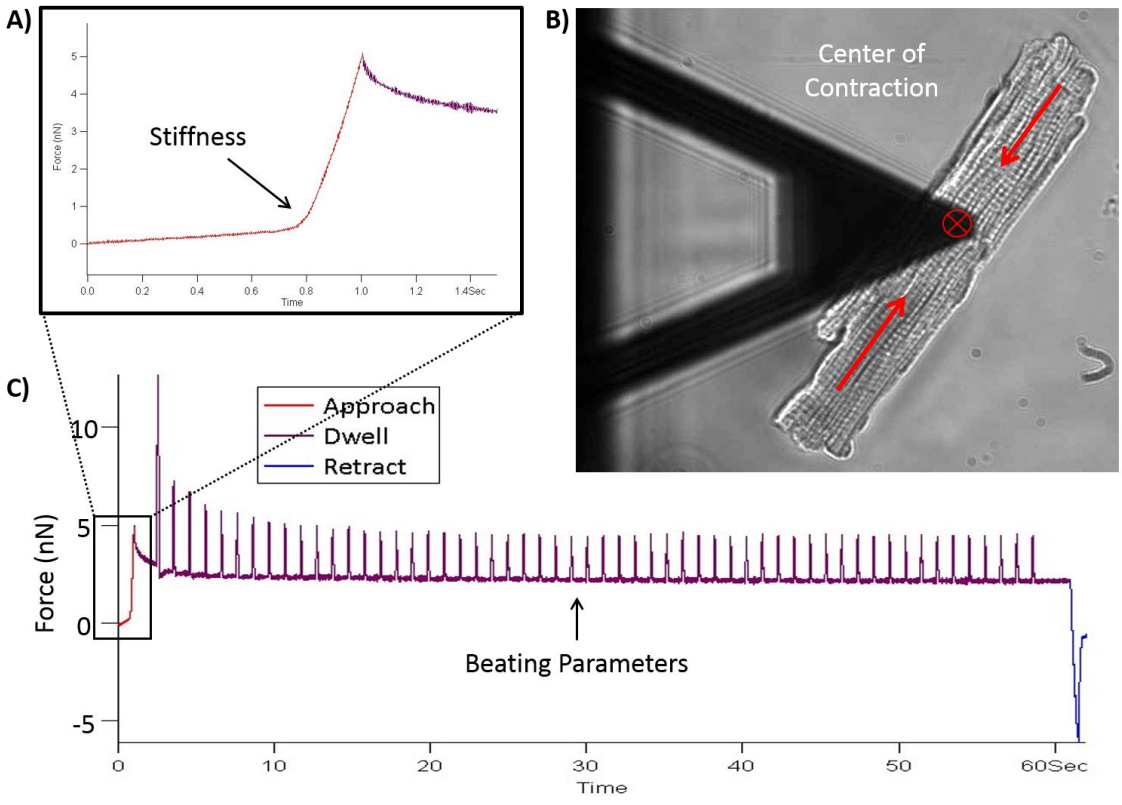

Figure 12. Sample data set using optimized protocol. A) Stiffness data was collected from the initial contact (approach) portion of the dwell curve. B) AFM tip alignment and positioning on the center of contraction. C) Full dwell curve demonstrating where stiffness and beating dynamics are extracted.

Additionally, data extraction from the "dwell" portion of dwell curves was performed using a multi-peak analysis package in the Igor software. An initial decay can be seen upon initiating stimulation, therefore the last 30 peaks were selected and fit individually to analyze the stable portion of the observed beating dynamics, automatically calculating the parameters of interest. This process can be seen in **Figure 13**, and allowed for statistical averaging to be done on each data set.

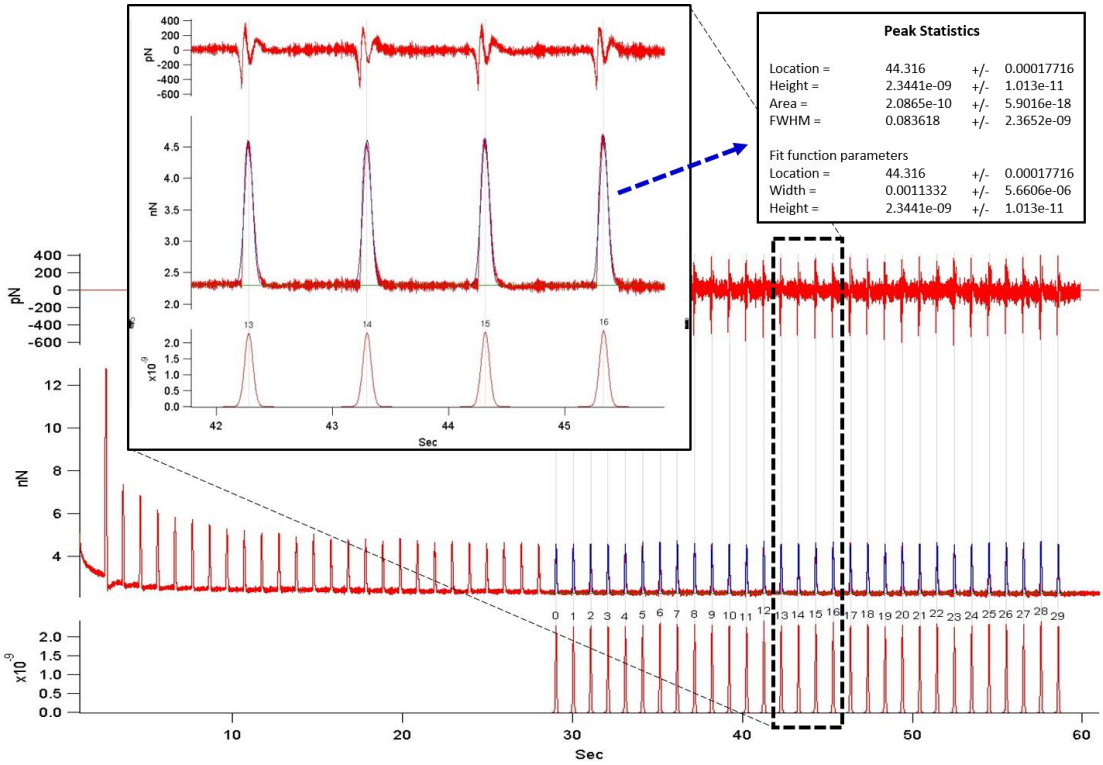

Figure 13. Multi-peak analysis of the last 30 peaks from the "dwell" portion of a dwell curve. Individual peaks are fit using the Igor software package, followed by the generation of peak statistics which allowed for the statistical averaging of each data set.

CHAPTER V

CARDIOMYOCYTE MECHANOBIOLOGY

In the following studies, we propose various experimental techniques to quantify the altered dynamics and mechanics associated with either a specific cardiomyopathy, in response to toxin exposure, or the eventual dysfunction caused by various stimuli including genetic modifications. Analyzing the cardiac cycle from the cellular level opens up new opportunities for characterizing pathophysiology, as well as enabling targeted studies of altered function in conjunction with previously known molecular variations representative of disease. The field of cardiomyocyte mechanobiology has clearly demonstrated the role that these physical parameters have on overall cardiac performance and cardiovascular health.

From a clinical perspective, the ability to prevent, diagnose, or treat patients suffering from a particular cardiomyopathy relies on an in-depth understanding of the different components involved. As more and more information is becoming available due to the advancement of genetic and molecular assays, some of the critical components involved in the molecular biology of different pathologies have provided enhanced therapeutic potential and better treatment options. Through this work, we aim to contribute to this understanding by quantifying the mechanobiological properties of cardiomyocytes with respect to various other factors, while examining these effects during cardiomyopathy, disease, pathophysiology, and toxin exposure. Upon combining the findings from this research with other well-established molecular techniques and

biomarkers, we can then further relate cellular studies with more physiologically relevant and translational research objectives.

Doxorubicin-Induced Cardiotoxicity

Doxorubicin is a known cardiotoxic agent, causing unwanted side effects when being used to treat various types of cancer. Because of this, it is important to determine the ways in which this and other drugs induce myocardial complications. The specific aim for this study was to analyze the effects of doxorubicin when introduced to individual cardiomyocytes. Using our advanced experimental platform, we were able to monitor the effects brought on by clinically relevant doses of this cardiotoxic compound. By monitoring the functional changes of individual cardiomyocytes upon the administration of drugs, we were then able to determine which aspects of the cardiac cycle are most vulnerable to this treatment in a time-dependent manner.

For this study, an integrated AFM/nanoindenter platform was used to study the pathophysiological effects that are associated with doxorubicin exposure. Using adult mouse ventricular myocytes, both control samples and doxorubicin treated samples were monitored over time for comparisons between each group of individual cardiomyocytes. As the changes were further analyzed, we were then able to look at which factors were ultimately affected in order to help identify which mechanisms are involved in doxorubicin-induced cardiotoxicity.

Anthracyclines, including doxorubicin, are among the most effective chemotherapeutic agents available for the treatment of several human cancers; however, their cardiotoxicity limits their clinical use. It has been reported that up to 60% of pediatric cancer patients will receive anthracycline treatment and that approximately 10% of those patients will develop symptomatic cardiomyopathy up to 15 years after the end of chemotherapy [18]. Due to the high incidence of associated cardiomyopathy, much work has been done to try and determine the specific mechanisms that are involved in doxorubicin cardiotoxicity, both acute and long-term.

There are several potential mechanisms that are thought to contribute to doxorubicin-induced cardiotoxicity, including ROS production, calcium overload, and metabolite toxicity. Most supporting evidence is able to address individual components of doxorubicin cardiotoxicity separately, but there remains to be a unifying accepted hypothesis that incorporates and explains all of the aspects of both acute and long-term damage occurring within the myocardium.

Initial experiments were performed by collecting beating dynamics using the AFM platform in order to monitor the response of individual cardiomyocytes to doxorubicin exposure. Ventricular cardiomyocytes were isolated from adult wild-type mice and immediately plated on petri dishes to maintain adult morphology and minimize the effects of long-term culture. Cells were stimulated at 1 Hz using platinum electrodes submerged within the petri dish and the threshold for inducing contractions was determined separately for each experiment (typically 4 ms pulse @ <20 V). At least

10 min of stable baseline measurements were collected and then 10 µm doxorubicin was added to the sample without altering the setup or the positioning of the AFM on the cell.

Data was collected as force versus time, with indentations being acquired at set intervals between beating data sets. Beating data was collected at 60 sec dwell intervals and the cantilever retracted between every data set. Stimulation was turned off between every dwell in order to ensure a reproducible contact force on the cell surface.

Initial results showed an increase, followed by a decrease, in the contraction force over a short time period (**Figure 14**). These initial findings helped to explain previous reports claiming either an increase or no change in contractility occurring in response to doxorubicin, which based on these results, could vary depending on experimental conditions and when the measurements were taken. However, the majority of studies have reported lowered contractility upon exposure to doxorubicin, which is more representative of the long-term physiological damage seen *in vivo* in animal studies and in human patients. This led to extending the time of exposure beyond 30 min to determine if other time-dependent changes could occur leading to an overall decrease in contractile force as seen from longer time studies.

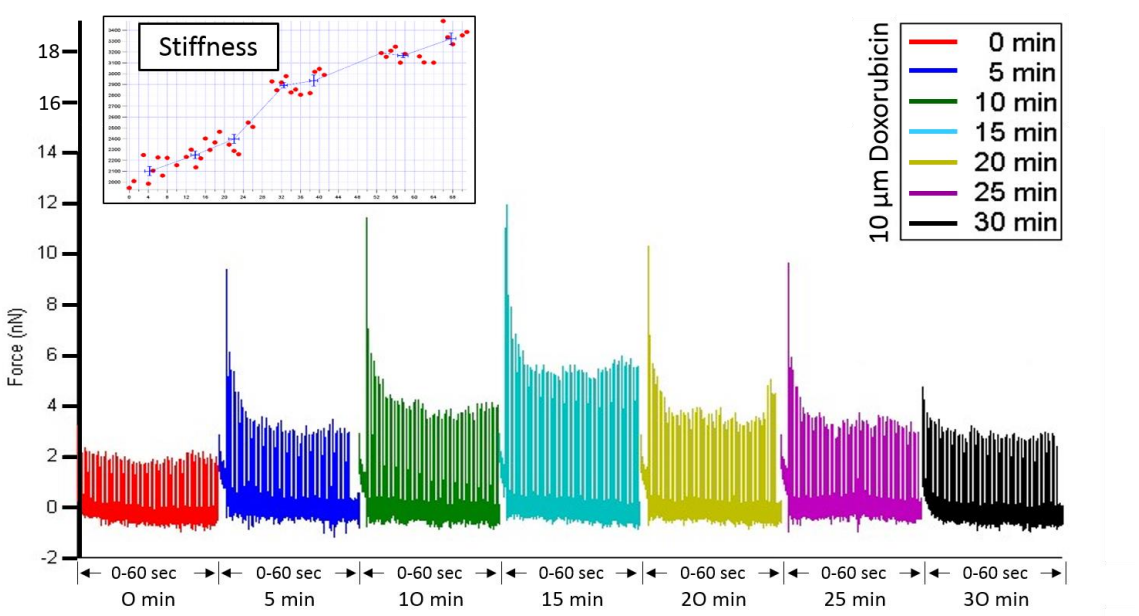

Figure 14. Initial contraction force data showing the response to 10 µm doxorubicin for up to 30 minutes of exposure, with stiffness data shown in inset.

A total of 10 mice were then used to gather both control (6 mice) and doxorubicin exposure (4 mice) data over an extended time period. The time taken for each experiment was approximately 2 hours and cells were only used within 6 hours of isolation, as it has been shown that changes can begin to occur after this time period which alter the adult cardiomyocyte morphology and could obscure the resulting data. Both control and doxorubicin samples were examined under identical settings and conditions for the same period of time, after which data was then combined and averaged for each group. To remove variations and allow comparisons to be made between cells, normalization for each cell was used to generate relative values for all of the parameters measured. Statistical analysis was then used at each time point to determine the significance between both data sets.

The relative force for samples treated with doxorubicin generated an average initial increase of +35% after 20 min of exposure (40 min), followed by an eventual average decrease of -39% after 90 min of exposure (110 min). Control samples maintained a relatively stable average force throughout the same duration of testing, only varying ±11% over time (**Figures 15-16**).

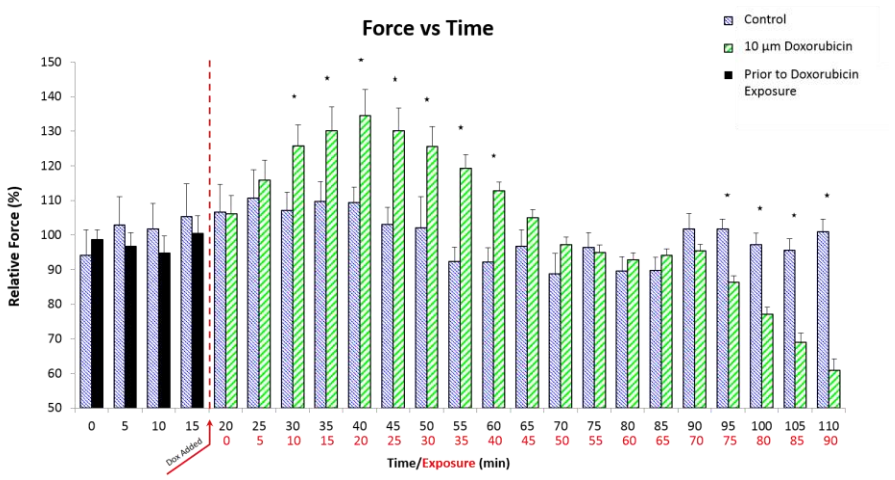

Figure 15. Time-course of force versus time for control and doxorubicin treated samples. Student's two-tailed t-test assuming an unequal variance was calculated using Microsoft® Excel to determine the statistical significance between control and doxorubicin treated samples at each time point. In all cases, a p value less than 0.05 was considered to be statistically significant (* $p < 0.05$).

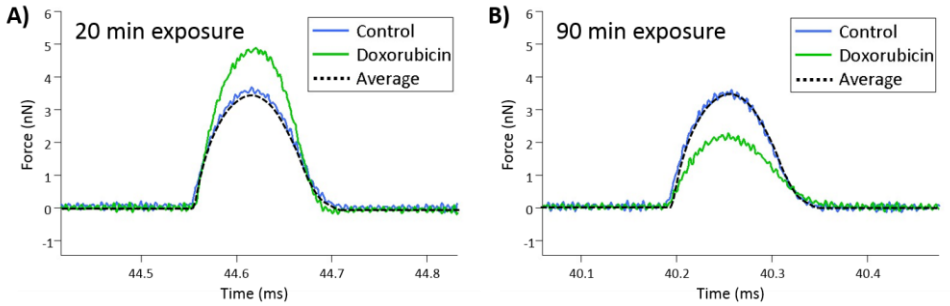

Avg. after 20 min	Control	Doxorubicin
Relative Force (%)	↑ 9.29 ± 5	↑ 34.55 ± 8

Avg. after 90 min	Control	Doxorubicin
Relative Force (%)	↑ 0.96 ± 4	↓ 39.13 ± 3

Figure 16. Individual representative peaks illustrating the relative force changes at the maximum and minimum time points in Figure 15. A) Representative peak and average data after 20 min of exposure. B) Representative peak and average data after 90 min of exposure.

The relative FWHM for samples treated with doxorubicin began generating a significant average increase after 35 min of exposure (55 min), peaking after around 80 min of exposure (100 min) at +14%. Control samples maintained a relatively stable FWHM, only varying ±4% over time (**Figures 17-18**).

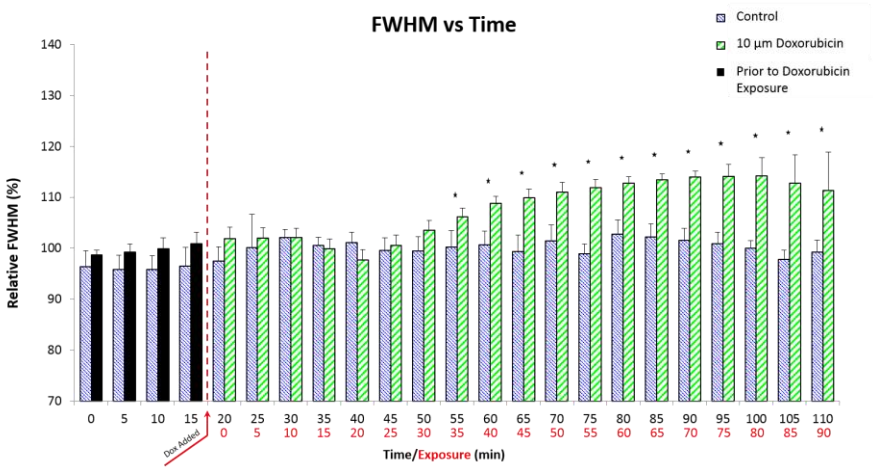

Figure 17. Time-course of FWHM versus time for control and doxorubicin treated samples. Student's two-tailed t-test assuming an unequal variance was calculated using Microsoft® Excel to determine the statistical significance between control and doxorubicin treated samples at each time point. In all cases, a p value less than 0.05 was considered to be statistically significant (* $p < 0.05$).

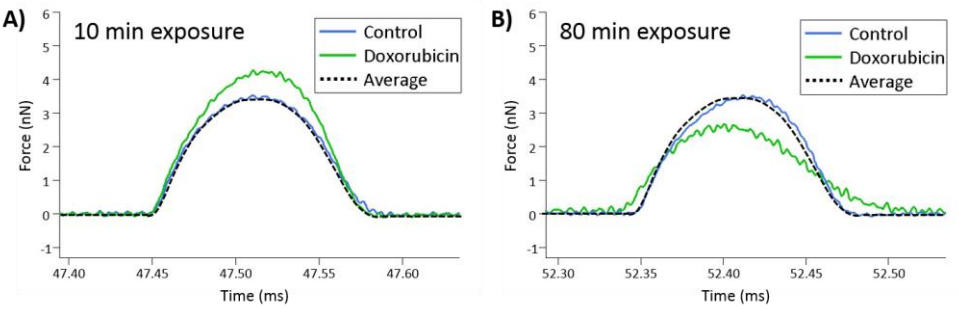

Avg. after 10 min	Control	Doxorubicin
Relative FWHM (%)	↑ 2.12 ± 2	↑ 2.05 ± 2

Avg. after 80 min	Control	Doxorubicin
Relative FWHM (%)	↑ 0.05 ± 1	↑ 14.17 ± 8

Figure 18. Individual representative peaks illustrating the relative FWHM changes at the maximum and close-to-baseline time points in Figure 17. A) Representative peak and average data after 10 min of exposure. B) Representative peak and average data after 80 min of exposure.

The relative stiffness for samples treated with doxorubicin showed an average initial increase by +21% over the first 30 min of exposure (50 min), matching control samples, but dropped back down to a stable value of only ±4% for the remainder of their exposure. Control samples, however, maintained a relatively steady average increase in stiffness over time peaking at +72%, when measurements were stopped (**Figures 19-20**).

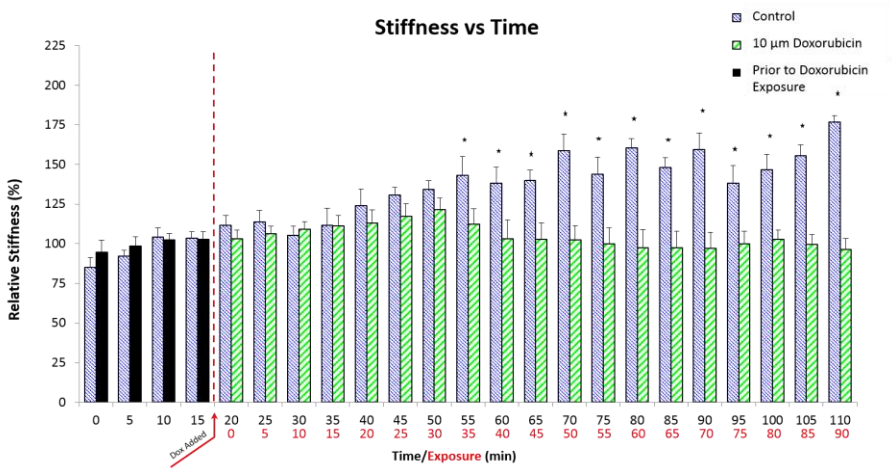

Figure 19. Time-course of stiffness versus time for control and doxorubicin treated samples. Student's two-tailed t-test assuming an unequal variance was calculated using Microsoft® Excel to determine the statistical significance between control and doxorubicin treated samples at each time point. In all cases, a p value less than 0.05 was considered to be statistically significant (* p < 0.05).

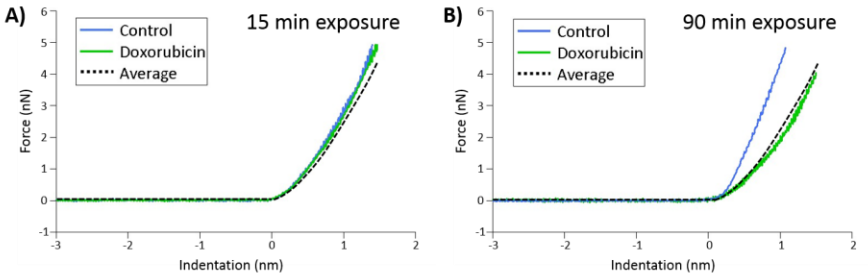

Avg. after 15 min	Control	Doxorubicin
Relative Stiffness (%)	↑ 11.59 ± 10	↑ 11.06 ± 5

Avg. after 90 min	Control	Doxorubicin
Relative Stiffness (%)	↑ 76.70 ± 5	↓ 3.70 ± 7

Figure 20. Individual force curves illustrating the relative stiffness changes from the maximum and close-to-baseline time points in Figure 19. A) Representative peak and average data after 15 min of exposure. B) Representative peak and average data after 90 min of exposure.

The initial acute response of cardiomyocytes is thought to be associated with doxorubicin exposure, but the eventual long-term response could point towards the increased accumulation and production of the major metabolite doxorubicinol within the cell. Other studies have shown that the long-term response appears to be unrelated to doxorubicin levels as it peaks very quickly, whereas doxorubicinol levels have been shown to increase significantly after 45 min of doxorubicin administration [19]. Intramyocardial metabolism of doxorubicin to doxorubicinol would help to explain the time-dependent response of cardiomyocytes, and the long-term effects seen in patients receiving treatment.

Other studies have reported inducing opposing effects on isolated cardiomyocytes when either doxorubicin or doxorubicinol was administered [20]. Doxorubicin-caused prolongation of action potential duration (APD) was thought to be the result of reduced Ca^{2+} extrusion via the Na^{+}/Ca^{2+} exchange and/or the prolonged Ca^{2+} influx via opening of Ca^{2+} channels. The doxorubicinol-caused shortening of APD was reported to be due to activation of I_k and partial depletion of sarcoplasmic reticulum (SR) Ca^{2+} content, both reducing the amount of Ca^{2+} available for myofilament activation during depolarization.

Results from the previous study also found opposing effects on cell shortening when cardiomyocytes were exposed to either doxorubicin or doxorubicinol [20]. Due to doxorubicin's inhibition of I_k tail currents and doxorubicinol's stimulation of I_k tail currents, APD was found to correlate directly with cell shortening. Therefore,

doxorubicin prolonged APD, increasing contractility and doxorubicinol decreased APD, reducing contractility.

Reactive oxygen species (ROS) production is also believed to play an important role in long-term doxorubicin-induced cardiotoxicity. Free radicals are known to impair sequestration of Ca^{2+} by the SR [21]. By promoting calcium release and the depletion of SR calcium stores, this action leads to impaired contractility by decreased supply of activator calcium and impaired cardiac relaxation by increased calcium at the myofibrils. An increase in Ca^{2+} concentration in the interior of myocardial fibers can cause damage to cell and organelle membranes by doxorubicin-generated oxygen radicals, leading to increased lipid peroxidation and membrane damage with the loss of membrane selective permeability. Additionally, increased oxidative stress is thought to promote apoptosis, as antioxidants have been shown to help inhibit this process. Mitochondrial injury and dysfunction are also key components involved in ROS damage [22]. Cardiomyocytes are rich in mitochondria, representing up to 50% of cardiomyocyte mass which serve as both source and target of ROS. Overall, depressed contractility is believed to be linked with malfunctioning SR Ca^{2+} release. As ryanodine receptors (RyRs) have a direct binding site for anthracyclines, this may interfere with proper Ca^{2+} handling and lead to inhibition. Other damage thought to be induced by ROS production include the degradation of myofilament and cytoskeletal proteins, and myofibrillar structural damage from doxorubicin-induced oxidative stress.

From this study, we were able to show a distinction between the initial and time-delayed response of individual cardiomyocytes upon doxorubicin exposure, illustrating the importance of time-dependence on the results and the improved monitoring capabilities of this platform over the time-course of exposure. It is proposed, and further supported by our findings, that the initial increase in force is likely due to the acute effects resulting from exposure to doxorubicin, while the eventual decrease in force, prolonged FWHM, and membrane damage are caused by the accumulation of the major metabolite doxorubicinol and its increased production of free radicals leading to oxidative stress. Based on supporting evidence from other studies, the likely causes for changes in contractility are linked to an increase or decrease in APD. Other mechanisms involved in the degradation of the cell membrane and an overall loss in contractility include SR Ca^{2+} dysfunction caused by anthracycline binding, mitochondrial damage both stemming from and propagating ROS production, and the deterioration of myofibrils due to an increase in free radicals within the cardiomyocyte.

While other studies are still needed to conclude the effects from both acute and long-term exposure to doxorubicin, these findings illustrate the potential for future treatment strategies aimed at targeting the eventual metabolism and downstream effects of doxorubicin. It was previously hypothesized that the mechanism of action which gives doxorubicin its cancer-fighting efficacy in cancer cells is separate from the mechanisms causing its cardiotoxicity in the heart. This work also supports this

hypothesis and points towards alternative strategies for mitigating the cardiotoxic effects of this drug without suppressing its chemotherapeutic potential.

Simulated Hypoxia

The goal for this specific aim was to quantitatively characterize the time-course of altered beating dynamics of adult mouse cardiomyocytes in response to simulated hypoxia. The resulting pathology associated with this event occurs when the level of oxygen drops below physiological levels, such as in ischemia, which causes myocardial damage upon an infarction. As this triggers a cascade of events which can lead to the loss of viable myocardial tissue and oxidative stress, it is important to determine both the time-course of degeneration and the underlying changes in cardiomyocyte mechanobiology as a result of these events.

In order to study the pathogenesis incurred during this process, an environmental chamber was used to regulate oxygen levels exposed to isolated adult mouse cardiomyocytes. The cells were subjected to hypoxic conditions (0.5% O_2), as the beating dynamics were constantly monitored in real-time throughout this process. Techniques illustrated above for acquiring cardiomyocyte beating dynamics through the utilization of DHM provided indicators of cell damage and altered performance. Various fluorescent markers indicative of ROS production were also used in additional experiments performed in conjunction with these to develop an understanding of the physio-chemical relationship that is induced upon this increased oxidative stress.

The results from this study show that there is an initial and gradual increase in both phase amplitude and the duration of contractions (**Figure 21**). The cardiomyocytes were only responsive to stimulation over the first 20 minutes of hypoxia. After 20 minutes, the contractions became erratic and spontaneous, without responding to stimulation as can be seen in the resulting phase versus time plots at the remaining time points (30-60 min). Another interesting result was the gradual increase in resting phase values over time as shown in **Figure 22**.

A)

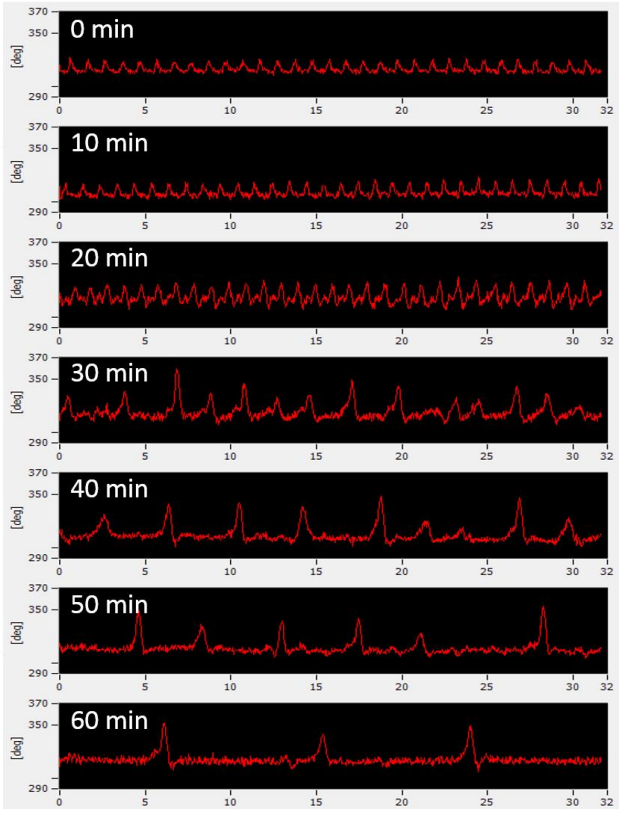

B)

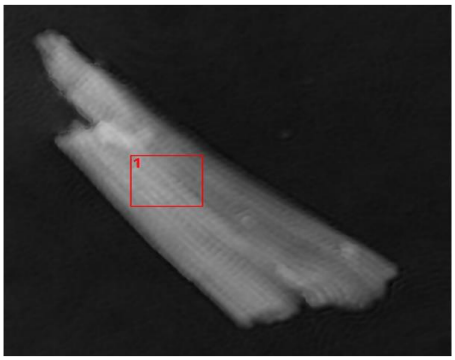

C)

Time (min)	Avg. Amplitude (deg)	Avg. Width (sec)
0	11.579 ± 1.346	0.455 ± 0.086
10	14.739 ± 1.652	0.517 ± 0.093
20	18.685 ± 1.687	0.558 ± 0.104
30	29.654 ± 8.359	0.943 ± 0.143
40	32.159 ± 9.062	0.964 ± 0.095
50	30.271 ± 6.913	0.925 ± 0.101
60	34.485 ± 5.659	0.977 ± 0.126

Figure 21. Phase monitoring of stimulated adult ventricular myocyte in response to simulated hypoxia. A) Phase versus time plots taken over the boxed region shown in (B). B) Phase image with region of interest selected for phase monitoring. C) Data analysis showing the average values for phase amplitude and peak duration over 60 minutes of exposure to hypoxic conditions.

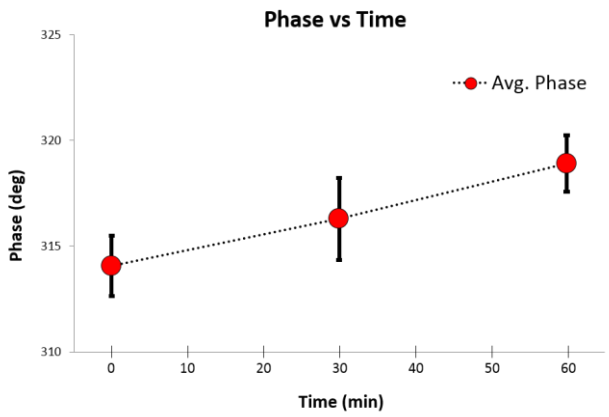

Figure 22. Average baseline phase value over time showing a gradual increase over 60 minutes of exposure to hypoxic conditions.

The gradual increase in average baseline phase could be due to the loss of selective permeability and altered calcium handling caused by membrane damage due to oxidative stress, along with the increased build-up and production of ROS. The initiation of arrhythmias and spontaneous activity also occurred between periods of quiescence, eventually leading to cell death. This represents the first study applying this phase monitoring technique to individual cardiomyocytes in response to hypoxic conditions. The mechanodynamic response coupled with the measured increase in ROS production along a similar time-scale illustrate the utility of this technique and also propose alternate strategies for detecting the increased production of ROS by monitoring phase changes within individual cardiomyocytes.

Wild-type vs Knockout

Genetic mutations for different proteins and components of excitation-contraction coupling can have a significant impact on the cardiac cycle and the overall

performance of the heart. While many studies have identified specific mutations leading to various types of cardiomyopathy, the exact mechanisms with which these changes cause damage can be difficult to identify. By using a knockout mouse model for a specific gene or protein of interest, we have been able to further characterize the changes that occur at the level of the cardiomyocyte and provide additional insight regarding the underlying mechanisms driving these changes. Analyzing isolated cardiomyocytes from both wild-type and transgenic mice, comparisons relating calcium dynamics and contractility were made to better assess the resulting altered mechanobiology.

Using our integrated AFM/LSCM platform, we performed a side-by-side comparison of cardiomyocytes from both wild-type and transgenic mice. Similar metrics were used to characterize the mechanobiological properties of each cell type in relation to calcium dynamics, while quantitative analyses of these metrics were then used to help identify those areas that were most effected by the induced alterations. As various molecular techniques have already provided data that can be used to help correlate these two components of cardiomyocyte behavior, we were able to utilize this information to help relate our findings with previous reports.

The resulting correlation between Ca^{2+} concentration and the contraction peak show that the alterations in beating dynamics are directly related to altered Ca^{2+} dynamics (**Figures 23-25**). Both parameters see a slight decrease in amplitude and a prolonged time-to-peak and time-to-relaxation in the knockout mouse model. These

results are able to confirm the overall effects that this particular mutation (an RyR specific protein) induces in this experimental mouse model. Mice suffering from this mutation exhibit impaired heart function showing dilated cardiomyopathy-like symptoms, such as decreased contractility, as well as the development of arrhythmias.

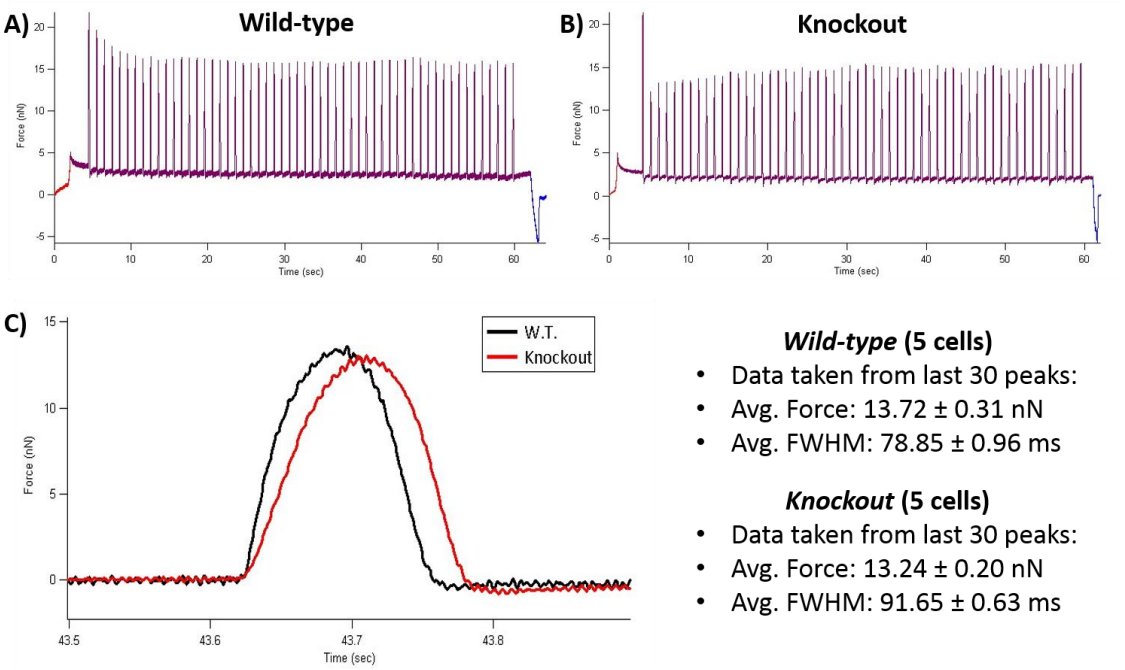

Figure 23. Dwell curves from wild-type and knockout cardiomyocytes. A) Wild-type dwell curve. B) Knockout dwell curve. C) Comparison of individual wild-type and knockout contraction peaks, along with statistics regarding average data taken from 5 cells of each type.

These results illustrate the advanced capabilities for this integrated platform to quantify mechanobiological changes in correlation with intracellular calcium dynamics. This also provides direct evidence for the cellular level changes associated with a specific mutation, opening up the potential for future studies and experimental mouse models of known genetic alterations of clinical importance.

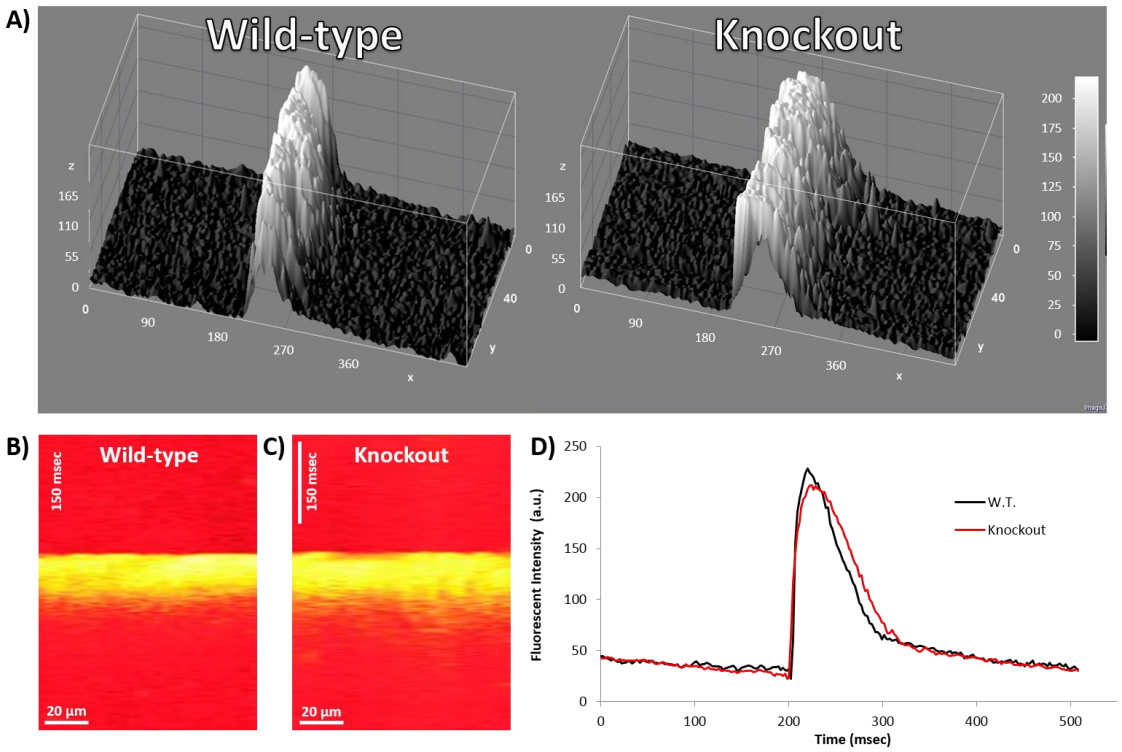

Figure 24. Calcium line-scan images from wild-type and knockout mice. A) 3D profile comparison of both cell types. B) Wild-type calcium line-scan. C) Knockout calcium line-scan. D) Comparison of wild-type versus knockout calcium line-scan profiles.

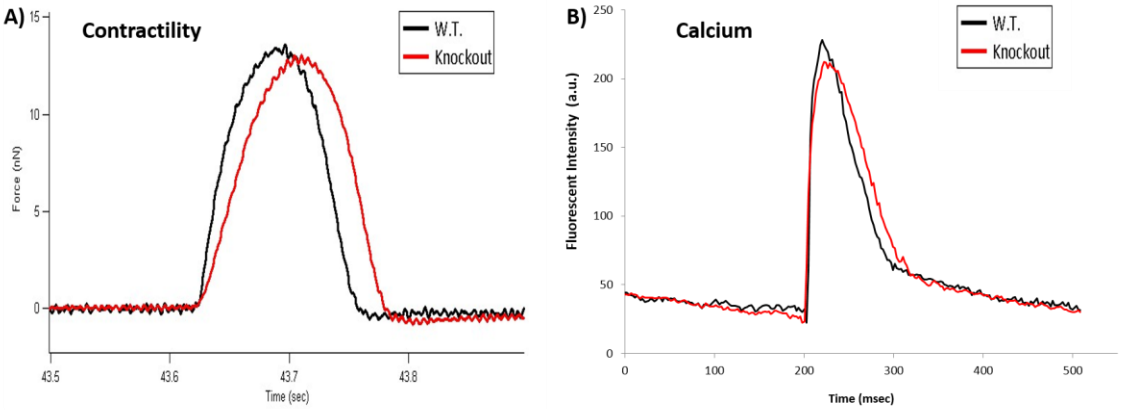

Figure 25. Contraction and calcium peaks showing a positive correlation. A) Contraction peaks of both cell types. B) Calcium dynamics from both cell types.

CHAPTER VI

STEM CELL MECHANOTRANSDUCTION

Stem cell applications with clinical significance have shown great potential for treating a variety of conditions. However, their limited success in clinical trials and the growing safety concerns associated with their use have stalled the development of new techniques and their overall impact in the medical field. As previously mentioned, some of the many challenges for this technology remain in the low cell retention rates upon implantation/injection and the inability to regulate and control their differentiation/integration within the host tissue. Although many studies have had success under *in vitro* conditions, the inability to recreate those results with *in vivo* applications has slowed the progress of this field, calling for a better understanding of the mechanisms responsible in regulating stem cell behavior.

Of the many areas currently under investigation, the role of mechanotransduction in stem cell biology has made several contributions. By quantifying the mechanical properties of these cells in response to various environmental conditions, we have been able to assess the importance of stiffness and physical cues upon stem cell differentiation and their potential influence for *in vivo* applications.

Mg53 Treatment

The role of physical stress on stem cell differentiation has drawn much interest and carries great potential for applications in tissue engineering and regenerative medicine. Varying levels and ranges of physical forces are present *in vivo* under physiological conditions depending on the cell types present within the tissue of interest. Recent studies have begun demonstrating the degree to which stem cells in particular respond to these mechanical cues. By quantifying the mechanical properties of these cells under varying conditions, we have been able to utilize membrane stiffness as a potential indicator of differentiation potential.

Using our integrated AFM/Nanoindenter platform, we have performed side-by-side comparisons of stem cell membrane stiffness upon exposure to Mg53 protein treatment. As this treatment is known to have a role in membrane repair and has been hypothesized to stimulate stem cell differentiation, we analyzed the resulting changes in membrane mechanics associated with this treatment. These studies have helped to further demonstrate the validity and relevance of studies regarding mechanotransduction, while utilizing a platform to better isolate the desired mechanical properties of interest and enabling future studies on this important relationship.

Mg53, a muscle-specific tripartite motif family protein of the membrane repair machinery, has a prominent in membrane repair [23], and has recently been linked with the stimulation of differentiation pathways. This study was interested in determining

whether or not this treatment affected membrane elasticity and differentiation potential in individual stem cells. A side-by-side comparison using nanoindentation was performed and preliminary data is shown in **Figure 26**. At both time points, Mg53 treated cells were found to have reduced stiffness and increased elasticity, although the difference becomes much more significant after 14 days in culture. Also, the percentage of differentiated cells undergoing Mg53 treatment was much larger than that of control samples.

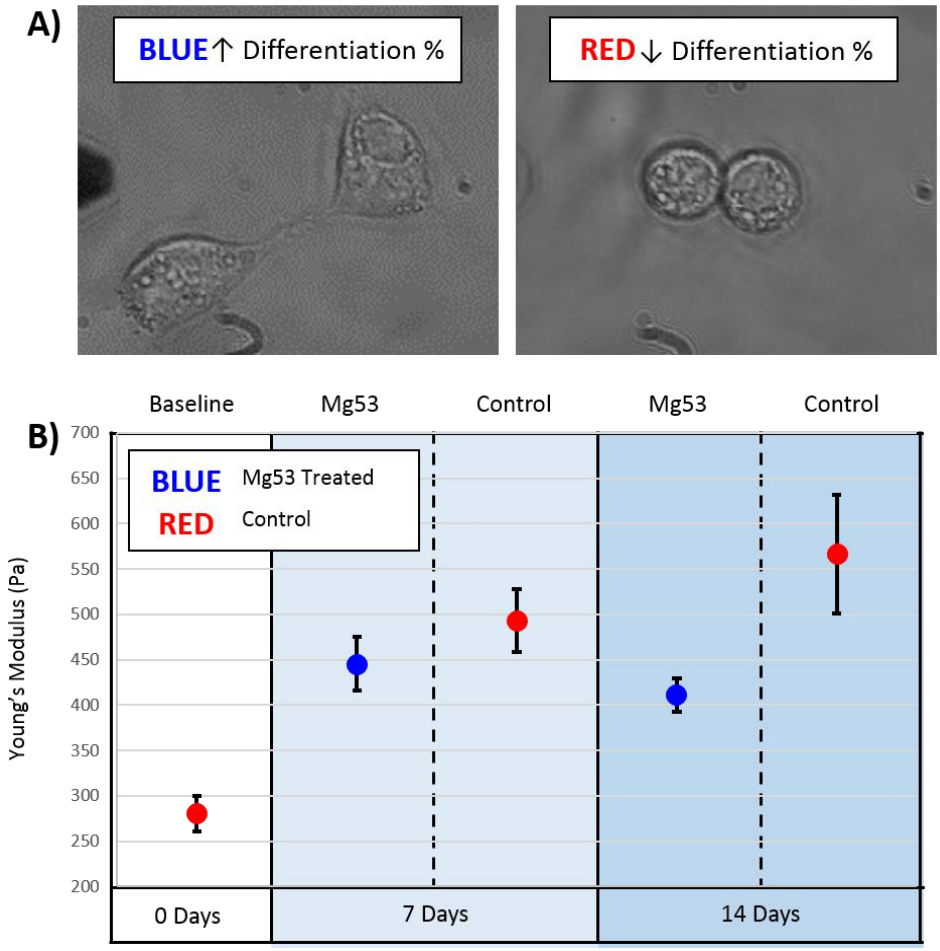

Figure 26. The effects of Mg53 treatment on differentiation and stiffness. A) Increased differentiation percentage between treated and non-treated cells. B) Stiffness measurements between treated and non-treated samples at 7 and 14 days.

Matrix Encapsulation

Using our integrated AFM/Nanoindenter platform, we have performed side-by-side comparisons of membrane stiffness for stem cell aggregates under encapsulation and those of bare aggregates in order to quantify the effects of a micromatrix coating on the resulting stiffness. These samples were further analyzed on their efficacy for treating myocardial infarction upon injection into the infarct zone by monitoring cell retention and successful integration within the host tissue. These studies also help to validate the significance of studies regarding mechanotransduction, while utilizing an advanced quantitative technique to better understand this important relationship.

As mentioned, one of the challenges facing stem cell therapy for myocardial infarction (MI) is the ability to maintain high cell retention *in vivo*. By encapsulating 3D stem cell aggregates in a biocompatible/biodegradable hydrogel micromatrix, researchers have been able to significantly enhance animal survival upon injection into the infarct zone.

Myocardial infarction (MI) is one of the leading causes of death [24, 25], due in part to the fact that the human heart has a very limited capacity to regenerate functional cardiac tissue after the loss of viable cells, particularly cardiomyocytes, following MI [26-28]. Several stem cell applications have shown promise as an option for treating MI, however, the reported retention percentages of stem cells in the infarct zone have been disappointing with as low as 1% of viable cells in the heart within a few

hours to days post injection [28-31]. The use of a core-shell architecture provided by matrix encapsulation mimics the physical configuration of embryos during the early stages of development and was an inspiration for the development of this coating procedure [32, 33].

Along with the obvious chemical factors and the optimization of diffusive properties of the matrix involved in accomplishing this effort, there was also an interest in seeing whether the physical properties of the matrix (or its stiffness) could play a role in successfully recreating physiological conditions for the injectable stem cell aggregates. By performing nanoindentation on prepared samples, we were able to show a significant difference between control groups without matrix encapsulation, and those cell aggregates that were subjected to matrix encapsulation (**Figure 27**).

These results offer an interesting hypothesis, suggesting that the mechanical cues supplied by the matrix could play a significant role in the successful implantation of stem cell aggregates in the heart, leading to a better overall integration within the host tissue and stimulating the differentiation of both cardiomyocytes and endothelial cells.

Supporting data collected in conjunction with this work was able to further show that the molecular dynamics of the stem cell aggregates were also altered upon matrix encapsulation, leading to the enhanced cell survival and retention upon injection. One of the additional components thought to provide increased efficacy was the temporary systemic immunosuppression provided by matrix encapsulation up to 6 days upon

injection, mitigating the potential for immune rejection during long-term studies [34-36]. This was thought to be due to the afforded immuno-isolation provided by the biodegradable matrix, leading to enhanced animal survival. Additionally, matrix encapsulation also significantly reduced fibrosis and improved cardiac function compared to control samples 15 days after injection.

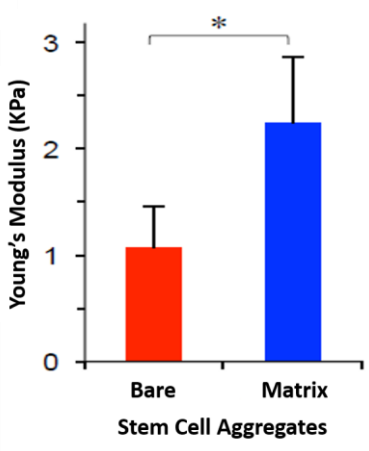

Figure 27. Comparison of Young's modulus between coated and non-coated stem cell aggregates.

Additional studies using GFP labeled cells also showed the ability of the injected cells to migrate through the MI zone while promoting their successful integration within the host tissue. The differentiation of a small percentage of injected cells towards endothelial cells was also shown to stimulate vasculogenesis and angiogenesis at the injection site. In summary, micromatrix encapsulation demonstrated its potential for clinical applications utilizing stem cell therapy, such as the successful treatment of MI, while illustrating the influence of physical cues on stem cell biology.

CHAPTER VII

FUTURE WORK AND CONCLUSIONS

Cardiomyocytes

Doxorubicin-Induced Cardiotoxicity

Through this study we were able to quantitatively characterize the time-dependent response of individual cardiomyocytes to doxorubicin exposure. We observed an acute increase in the force of contraction followed by an eventual decrease in contractility, a time-dependent increase in FWHM, and a relative decrease in membrane stiffness over time. These time-dependent responses appear to be due to the metabolism of doxorubicin into doxorubicinol, along with the increased production of ROS and subsequent membrane damage.

Future studies of doxorubicin-induced cardiotoxicity will incorporate additional components and inhibitors to try and further isolate the time-dependent effects in response to doxorubicin/doxorubicinol exposure. This includes the time-course of cardiomyocyte exposure to doxorubicinol, as well as, the combined treatment with an antioxidant such as Vitamin C.

Simulated Hypoxia

Through this study we were able to monitor the time-dependent dynamic response of individual cardiomyocytes to hypoxic conditions. We observed a slight initial increase in contractility and beat duration, followed by the generation of

spontaneous activity and the inability to stimulate periodic contractions. An overall increase in the baseline phase between contractions was also observed, potentially correlating with an increase in ROS and an altered intracellular refractive index.

Future work using the DHM to study simulated hypoxia will utilize the integrated fluorescence module, along with the dynamic characterization of cardiomyocyte contractility. Combining the detection and calculation of ROS production directly with altered mechanodynamics will help to better represent the time-course of damage, along with the potential for combining various therapeutic strategies and treatments aimed at mitigating this response. Altering the time of exposure to hypoxic conditions, followed by its subsequent reoxygenation, will allow for the determination of the time window for optimizing cell recovery in combination with potential treatments.

Wild-type vs Knockout

Through this study we were able to perform a side-by-side comparison of individual cardiomyocytes in order to directly measure the effects of a specific mutation on cardiomyocyte contractility. We observed a decrease in the force of contraction and an increase in beat duration in the knockout cells relative to wild-type cardiomyocytes. A comparison of the calcium-contraction relationship further supported these findings, illustrating the capabilities of this platform to quantify and relate subtle changes in cardiomyocyte contractility and calcium dynamics.

Extending studies towards a variety of genetically altered mouse models opens up the possibilities for mapping out the direct effects for a particular protein, or group of proteins, having a known association with a specific cardiomyopathy of interest. While initial results have demonstrated the potential for these types of studies, there still remains a large percentage of genetic mutations that have not been traced to their influence regarding a specific mechanism at the cellular level.

Stem Cells

Mg53 Treatment

With this study we were able to investigate the effects of Mg53 treatment on stem cell differentiation, and the potential role that membrane elasticity has on this relationship. We observed a slight decrease in membrane rigidity upon 7 days of treatment with Mg53; however, a much more significant reduction in this measurement was attained after 14 days in culture relative to control samples. Using nanoindentation, the increased differentiation of stem cells treated with Mg53 showed a direct correlation with membrane elasticity. These findings lead to the hypothesis that membrane stiffness could serve as a potential indicator of differentiation potential in stem cells, with increased elasticity enabling the differentiation of stem cells by stimulating rapid attachment and promoting phenotypic changes upon treatment in culture.

Additional studies on stem cell mechanics include the effects of a freeze-thawing cycle. While cryopreservation is a commonly used method for storing and culturing various cell types, the effects that this process may have on membrane stiffness, and ultimately stem cell differentiation, have not been examined.

Matrix Encapsulation

Through this study, we were able to demonstrate that stem cell aggregates treated by matrix encapsulation leads to an increase in Young's modulus compared to bare stem cell aggregates. Further studies completed by collaborators found an overall enhancement in cell retention and tissue integration upon injection of the matrix encapsulated aggregates into the infarct zone of MI mouse hearts. This correlation in stiffness and successful implantation leads to the hypothesis that the physical cues imposed by the matrix better mimic in vivo conditions, which could lead to the improved efficacy of stem cell treatments.

Further quantification of the physiological forces that occur during embryogenesis could lead to the optimization of this technique, enabling the recreation of specific mechanical cues *in vitro* by tailoring the material properties of the hydrogel matrix and better mimicking those found *in vivo.* These studies will also be extended to various other tissue regeneration applications and stem cell therapeutics.

Summary

In conclusion, this work includes the use of new and innovative techniques to quantitatively analyze cardiomyocyte mechanodynamics and the role of stem cell mechanics under various experimental conditions. This research addresses key components of cardiovascular research that are currently still largely unknown, and has the potential for clinical implications regarding prognosis, treatment, and the prevention of various cardiomyopathies. Also, as stem cell therapies become more advanced, there will be a growing need for the development of similar techniques in order to quantify the physical mechanisms of differentiation in association with the complex network of molecular signaling.

LIST OF REFERENCES

1. Tardiff, J.C., *Cardiac hypertrophy: stressing out the heart.* The Journal of Clinical Investigation, 2006. **116**(6): p. 1467-1470.
2. Houser, S.R. and K.B. Margulies, *Is Depressed Myocyte Contractility Centrally Involved in Heart Failure?* Circulation Research, 2003. **92**(4): p. 350-358.
3. Chang, W.-T., et al., *Characterization of the Mechanodynamic Response of Cardiomyocytes with Atomic Force Microscopy.* Analytical Chemistry, 2012. **85**(3): p. 1395-1400.
4. Liu, J., et al., *Atomic Force Mechanobiology of Pluripotent Stem Cell-Derived Cardiomyocytes.* PLoS ONE, 2012. **7**(5): p. e37559.
5. Brady, A.J., *Mechanical properties of isolated cardiac myocytes.* Physiological Reviews, 1991. **71**(2): p. 413-428.
6. Azeloglu, E. and K. Costa, *Atomic Force Microscopy in Mechanobiology: Measuring Microelastic Heterogeneity of Living Cells*, in *Atomic Force Microscopy in Biomedical Research*, P.C. Braga and D. Ricci, Editors. 2011, Humana Press. p. 303-329.
7. Domke, J., et al., *Mapping the mechanical pulse of single cardiomyocytes with the atomic force microscope.* European Biophysics Journal, 1999. **28**(3): p. 179-186.
8. Bers, D.M., *Cardiac excitation-contraction coupling.* Nature, 2002. **415**(6868): p. 198-205.
9. Fabiato, A., *Calcium-induced release of calcium from the cardiac sarcoplasmic reticulum*. Vol. 245. 1983. C1-C14.
10. Sheehy, S., A. Grosberg, and K. Parker, *The contribution of cellular mechanotransduction to cardiomyocyte form and function.* Biomechanics and Modeling in Mechanobiology, 2012. **11**(8): p. 1227-1239.
11. Engler, A.J., et al., *Matrix Elasticity Directs Stem Cell Lineage Specification.* Cell, 2006. **126**(4): p. 677-689.
12. Evans, N.D., et al., *Substrate Stiffness Affects Early Differentiation Events in Embryonic Stem Cells.* Journal of European Cells and Materials, 2009. **18**: p. 1-14.
13. Obokata, H., et al., *Stimulus-triggered fate conversion of somatic cells into pluripotency.* Nature, 2014. **505**(7485): p. 641-647.
14. Ikehara, S., *Grand Challenges in Stem Cell Treatments.* Frontiers in Cell and Developmental Biology, 2013. **1**.
15. *Dynamic micromechanical properties of cultured rat atrial myocytes measured by atomic force microscopy*, ed. S.G. Shroff, D.R. Saner, and R. Lal. Vol. 269. 1995. C286-C292.
16. Helm, P., O. Franksson, and K. Carlsson, *A confocal scanning laser microscope for quantitative ratiometric 3D measurements of [Ca2+] and Ca2+ diffusions in living cells stained with Fura-2.* Pflügers Archiv, 1995. **429**(5): p. 672-681.

17. Fiset, C., et al., *A rapidly activating sustained K+ current modulates repolarization and excitation-contraction coupling in adult mouse ventricle.* The Journal of Physiology, 1997. **504**(Pt 3): p. 557-563.
18. Octavia, Y., et al., *Doxorubicin-induced cardiomyopathy: From molecular mechanisms to therapeutic strategies.* Journal of Molecular and Cellular Cardiology, 2012. **52**(6): p. 1213-1225.
19. Olson, R.D., et al., *Doxorubicin cardiotoxicity may be caused by its metabolite, doxorubicinol.* Proceedings of the National Academy of Sciences, 1988. **85**(10): p. 3585-3589.
20. Wang, Y.-X. and M. Korth, *Effects of Doxorubicin on Excitation-Contraction Coupling in Guinea Pig Ventricular Myocardium.* Circulation Research, 1995. **76**(4): p. 645-653.
21. Wenzel, D.G., *Drug-induced cardiomyopathies.* Journal of Pharmaceutical Sciences, 1967. **56**(10): p. 1209-1224.
22. Olson, R.D. and P.S. Mushlin, *Doxorubicin cardiotoxicity: analysis of prevailing hypotheses.* The FASEB Journal, 1990. **4**(13): p. 3076-86.
23. Weisleder, N., et al., *Recombinant MG53 Protein Modulates Therapeutic Cell Membrane Repair in Treatment of Muscular Dystrophy.* Science Translational Medicine, 2012. **4**(139): p. 139ra85.
24. Go, A.S., et al., *Heart disease and stroke statistics--2013 update: a report from the American Heart Association.* Circulation, 2013. **127**(1): p. e6-e245.
25. Laslett, L.J., et al., *The worldwide environment of cardiovascular disease: prevalence, diagnosis, therapy, and policy issues: a report from the American College of Cardiology.* Journal of the American College of Cardiology, 2012. **60**(25 Suppl): p. S1-49.
26. Segers, V.F. and R.T. Lee, *Stem-cell therapy for cardiac disease.* Nature, 2008. **451**(7181): p. 937-42.
27. Laflamme, M.A. and C.E. Murry, *Heart regeneration.* Nature, 2011. **473**(7347): p. 326-35.
28. Sanganalmath, S.K. and R. Bolli, *Cell therapy for heart failure: a comprehensive overview of experimental and clinical studies, current challenges, and future directions.* Circ Res, 2013. **113**(6): p. 810-34.
29. Christoforou, N., et al., *Implantation of mouse embryonic stem cell-derived cardiac progenitor cells preserves function of infarcted murine hearts.* PloS one, 2010. **5**(7): p. e11536.
30. Vunjak-Novakovic, G., et al., *Challenges in cardiac tissue engineering.* Tissue engineering. Part B, Reviews, 2010. **16**(2): p. 169-87.
31. Hirt, M.N., A. Hansen, and T. Eschenhagen, *Cardiac tissue engineering: state of the art.* Circulation research, 2014. **114**(2): p. 354-67.
32. Lewis, R., et al., *Human Reproduction and Development (Chapter 40)*, in *Life (5th Ed.)*. 2004, McGraw-Hill Higher Education: Columbus, OH.

33. Scadden, D.T., *The stem-cell niche as an entity of action.* Nature, 2006. **441**(7097): p. 1075-9.
34. de Almeida, P.E., et al., *Immunogenicity of pluripotent stem cells and their derivatives.* Circulation research, 2013. **112**(3): p. 549-61.
35. Pearl, J.I., et al., *Short-term immunosuppression promotes engraftment of embryonic and induced pluripotent stem cells.* Cell stem cell, 2011. **8**(3): p. 309-17.
36. Zhao, T., et al., *Immunogenicity of induced pluripotent stem cells.* Nature, 2011. **474**(7350): p. 212-5.

VITA

Ben Reese was born in Union City, TN, to the parents of Ed and Rosemary Reese. He is the second of four children: Katie, Will, and Sarah. Ben attended Lake Road Elementary and continued to Union City High School in Union City, Tennessee. After graduation, he headed to the University of Tennessee at Knoxville to pursue Biomedical Engineering. He completed his Bachelors of Science degree from the University of Tennessee in May 2009. Ben then accepted a graduate research assistantship at Oak Ridge National Lab where he completed his Masters of Science degree in Biomedical Engineering at the University of Tennessee in May 2011. He further continued his research by accepting a graduate research/teaching assistantship, and finished his Doctor of Philosophy degree in Biomedical Engineering from the University of Tennessee in December 2014.